Hearing Research 439 (2023) 108895

Contents lists available at ScienceDirect

Hearing Research

journal homepage: www.elsevier.com/locate/heares

Research Paper

The efficacy of a TrkB monoclonal antibody agonist in preserving the auditory nerve in deafened guinea pigs

Henk A. Vink [a,b], Dyan Ramekers [a,b], Alan C. Foster [c], Huib Versnel [a,b,*]

[a] Department of Otorhinolaryngology and Head & Neck Surgery, University Medical Center Utrecht, Utrecht University, Room G.02.531, P.O. Box 85500, 3508 GA, Utrecht, the Netherlands
[b] UMC Utrecht Brain Center, Utrecht University, Utrecht, the Netherlands
[c] Otonomy Inc., San Diego, CA, USA

ARTICLE INFO

Keywords:
cochlea
Hearing loss
Neurodegeneration
Spiral ganglion cell
eCAP
IPG effect
Neuroprotection
neurotrophic factor
TrkB receptor agonist

ABSTRACT

The auditory nerve typically degenerates following loss of cochlear hair cells or synapses. In the case of hair cell loss neural degeneration hinders restoration of hearing through a cochlear implant, and in the case of synaptopathy suprathreshold hearing is affected, potentially degrading speech perception in noise. It has been established that neurotrophins such as brain-derived neurotrophic factor (BDNF) and neurotrophin-3 (NT-3) can mitigate auditory nerve degeneration. Several potential BDNF mimetics have also been investigated for neurotrophic effects in the cochlea. A recent *in vitro* study showed favorable effects of M3, a TrkB monoclonal antibody agonist, when compared with BDNF. In the present study we set out to examine the effect of M3 on auditory nerve preservation *in vivo*. Thirty-one guinea pigs were bilaterally deafened, and unilaterally treated with a single 3-μl dose of 7 mg/ml, 0.7 mg/ml M3 or vehicle-only by means of a small gelatin sponge two weeks later. During the experiment and analyses the experimenters were blinded to the three treatment groups. Four weeks after treatment, we assessed the treatment effect (1) histologically, by quantifying survival of SGCs and their peripheral processes (PPs); and (2) electrophysiologically, with two different paradigms of electrically evoked compound action potential (eCAP) recordings shown to be indicative of neural health: single-pulse stimulation with varying inter-phase gap (IPG), and pulse-train stimulation with varying inter-pulse interval. We observed a consistent and significant preservative effect of M3 on SGC survival in the lower basal turn (approximately 40% more survival than in the untreated contralateral cochlea), but also in the upper middle and lower apical turn of the cochlea. This effect was similar for the two treatment groups. Survival of PPs showed a trend similar to that of the SGCs, but was only significantly higher for the highest dose of M3. The protective effect of M3 on SGCs was not reflected in any of the eCAP measures: no statistically significant differences were observed between groups in IPG effect nor between the M3 treatment groups and the control group using the pulse-train stimulation paradigm. In short, while a clear effect of M3 was observed on SGC survival, this was not clearly translated into functional preservation.

1. Introduction

Deafness in most cases is caused by severe loss of hair cells in the cochlea. In deaf subjects hearing can be partially restored with a cochlear implant (CI) by electrically stimulating the auditory nerve, bypassing the hair cells. The spiral ganglion cells (SGCs), which make up the auditory nerve, degenerate following deafness presumably due to lack of neurotrophic support from the organ of Corti (Ylikoski et al., 1974; Spoendlin, 1975; Webster and Webster, 1981; Leake and Hradek, 1988; Staecker et al., 1996; Shepherd and Hardie, 2001; Versnel et al., 2007; Ramekers et al., 2012 [Review]; Zilberstein et al., 2012). There is evidence that this degeneration negatively affects the benefits of a CI (Seyyedi et al., 2014; Kamakura and Nadol, 2016). The auditory nerve may also degenerate after loss of synapses while the inner hair cells remain intact (Kujawa and Liberman, 2015). This phenomenon of synaptopathy, caused by noise exposure and/or aging, negatively affects suprathreshold hearing while hearing thresholds remain normal (Wu et al., 2021), which is also known as hidden hearing loss (HHL). Many

* Corresponding author at: Department of Otorhinolaryngology and Head & Neck Surgery, University Medical Center Utrecht, Utrecht University, Room G.02.531, P.O. Box 85500, 3508 GA, Utrecht, the Netherlands.
E-mail address: H.VERSNEL@UMCUTRECHT.NL (H. Versnel).

https://doi.org/10.1016/j.heares.2023.108895
Received 8 February 2023; Received in revised form 31 August 2023; Accepted 2 October 2023
Available online 4 October 2023

studies have already shown that treatment with neurotrophic factors, such as brain-derived neurotrophic factor (BDNF), can prevent SGC degeneration (e.g. Ernfors et al., 1996; Miller et al., 1997, 2007; Gillespie et al., 2004; Shepherd et al., 2005; Wise et al., 2005, 2016; Glueckert et al., 2008; Agterberg et al., 2009; Landry et al., 2011; Budenz et al., 2015; Havenith et al., 2015; Sly et al., 2016; Scheper et al., 2020) and loss of nerve responsiveness (e.g. Ramekers et al., 2015a; Vink et al., 2020, 2022). Several groups have investigated molecules that activate TrkB, the receptor that mediates BDNF's neurotrophic effects, for beneficial effects in the cochlea and other tissues (Jang et al., 2010a,b,c; Massa et al., 2010; Liu et al., 2010; Longo and Massa, 2013; Yang et al., 2016; Szobota et al., 2019; Vink et al., 2020; Brahimi et al., 2021). These studies led to the discovery of several different promising BDNF mimetics (e.g. the small molecules 7,8'-DHF, 7,8,3'-THF, Deoxygedunin, LM22A4 and LM22B10, engineered neurotrophins with dual TrkB and TrkC agonist activity and monoclonal antibodies) with varying degrees of success. For instance, the small molecule 7-8-3'-THF was shown to be able to be able to protect SGCs in mice both *in vitro* and *in vivo*, exceeding the effectiveness of BDNF (Yu et al., 2012, 2013), while this effect was not observed *in vivo* in guinea pigs (Vink et al., 2020).

The mechanism by which BDNF and NT-3 exert their neurotrophic effects is complex (Huang and Reichardt, 2001; Chao, 2003; Saragovi et al., 2019). Acute activation of cell surface Trk receptors induces numerous intracellular signaling cascades in neurons (Huang and Reichardt, 2003). In addition, Trk receptor internalization and long range signaling via the intracellular "signaling endosome" can regulate long-term changes in gene expression (Howe and Mobley, 2004; Bronfman et al., 2007). BDNF has also been shown to induce its own synthesis from neurons, setting up a virtuous cycle (Canossa et al., 1997), also referred to as autocrine loop (Ramekers et al., 2012, 2015a). BNDF and NT-3 also have the ability to activate the p75 neurotrophin receptor ($p75^{NTR}$) that mediates effects, including apoptosis, that can oppose the neurotrophic effects of Trk receptor activation (Saragovi et al., 2019). Finally, acute versus chronic exposure to neurotrophins can produce markedly different neuronal responses (Ji et al., 2010). These factors raise uncertainty regarding any prediction of the effects of neurotrophins on a given cellular system. The effects of BDNF and NT-3 on the survival, neurite outgrowth and synaptogenesis in spiral ganglion neurons have been well documented (Fritzsch et al., 2004; Ernfors et al., 1996; Miller et al., 1997, 2007; Gillespie et al., 2004; Shepherd et al., 2005; Wise et al., 2005, 2016; Glueckert et al., 2008; Agterberg et al., 2009; Landry et al., 2011; Green et al., 2012; Budenz et al., 2015; Havenith et al., 2015; Ramekers et al., 2015a; Sly et al., 2016; Scheper et al., 2020; Szobota et al., 2019; Vink et al., 2020). Within the cochlea, tonotopic gradients of these neurotrophins exist and change during the stages of development and likely influence the differential properties of SGCs along the tonotopic axis. In general, BDNF expression has been associated with a base to apex gradient with the opposite orientation for NT-3 (Green et al., 2012; Sugawara et al., 2007). However, in adulthood, the levels of endogenous BDNF and NT-3 are markedly reduced (Green et al., 2012; Sugawara et al., 2007). Nonetheless, TrkB and TrkC receptors are present and apparently co-expressed in all SGNs, with no evidence for a tonotopic gradient during development (Green et al., 2012; Kersigo et al., 2018), although a base to apex gradient for TrkB mRNA may emerge in adulthood (Schimmang et al., 2003). Consequently, exogenously-applied Trk receptor agonists have the potential to have therapeutic benefit across the cochlear length, and in the adult the effects of TrkB agonists may be biased towards the basal cochlea. This indicates that the ability of BDNF mimetics to provide similar or improved neurotrophic effects in the cochlea is not straightforward and may depend on multiple factors including mode of TrkB activation, pharmacokinetics and disposition within cochlea tissues; as such, thorough testing of potential BDNF mimetics is warranted.

Previous studies in our model had indicated that BDNF gave the best efficacy across the agents tested (Vink et al., 2020, 2022). For the present experiments, we chose to study M3 as an optimized, potent and highly selective TrkB agonist, which has shown neurotrophic effects on spiral ganglion neurons *in vitro* in terms of survival, neurite outgrowth and synapse restoration (Szobota et al., 2019). M3 has no measurable affinity for TrkC receptors and, unlike BDNF, does not bind to $p75^{NTR}$. In addition, since M3 is a monoclonal antibody, it was reasonable to assume that its biological half-life would exceed that of the endogenous neurotrophins that are known to be easily broken down *in vivo* and therefore had the potential to achieve a greater effect than BDNF. Use of M3 allowed us to evaluate whether a truly selective TrkB agonist would be superior in its effects to BDNF. In the present study we aimed to investigate the *in vivo* preservative effect on the auditory nerve of treatment with the monoclonal antibody M3. To this end, a guinea pig model of ototoxicity-induced deafness was used, in which M3 was administered using gelatin-sponge-mediated delivery (Vink et al., 2020). The effect of M3 was analyzed in terms of quantified neural survival and electrophysiological responsiveness. In addition to the quantification of SGC somata as a measure of auditory nerve survival, their peripheral processes (PPs) are increasingly used as a measure of SGC survival, health and function (Wise et al., 2005; Glueckert et al., 2008; Waaijer et al., 2013; Ramekers et al., 2020; Vink et al., 2021) as these fibers are the site of excitation for the SGCs and are likely to be important for electrical stimulation. In addition, the PPs, and in particular their ribbon synapses, are a subject of growing interest due to synaptopathy being the basis of HLL (for review, see Foster et al., 2022). Therefore, the potential of PP preservation is also an important criterion for neuroprotective drugs in the cochlea. We used two distinct electrically evoked compound action potential (eCAP) stimulation paradigms to electrophysiologically assess neural health after treatment with M3: the single-pulse inter-phase gap (IPG) paradigm (Prado-Guitierrez et al., 2006; Ramekers et al., 2014, 2015a, 2022) and the pulse-train paradigm (Ramekers et al., 2015b).

Treatment with BDNF, using the same delivery method (i.e. with gelfoam), had resulted in significant SGC soma preservation predominantly in the basal turn of the cochlea combined with functional preservation (Havenith et al., 2015; Vink et al., 2020; 2022). Since *in vitro* application of M3 resulted in a preservative effect similar to that of BDNF (Szobota et al., 2019), we expected to find *in vivo* SGC preservation in at least the cochlear basal turn and, because of the theoretically superior biostabilty of the antibody, possibly in the middle and apical turns as well.

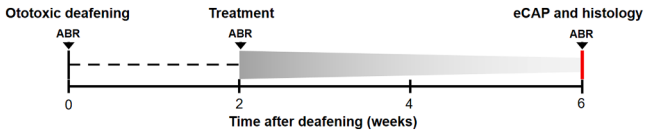

Fig. 1. Schematic overview of the experiment, adapted from Vink et al. (2020); their Fig. 1. On day 0, the animals were deafened via a co-administration of furosemide and kanamycin. Two weeks following deafening, the animals received the treatment by means of a gelatin sponge placement on the round window membrane. Treatments were 3 μl of 7 mg/ml M3 in buffer ($M3_{HI}$, n = 10), 3 μl of 0.7 mg/ml M3 in buffer ($M3_{LO}$, n = 11), or 3 μl buffer without M3 ($M3_{NO}$, n = 10). Four weeks after treatment, electrophysiological recordings were performed, after which the cochleas were harvested and processed for histological analysis.

2. Methods

2.1. Animals and experimental overview

For the present study, thirty-one adult female guinea pigs (Dunkin Hartley; Hsd Poc:DH; 250-350 g) were obtained from Envigo (Horst, the Netherlands) after which they were kept under standard laboratory conditions (light-on cycle: 07:00 AM-07:00 PM; *ad libitum* food and water; temperature of 21°C; humidity 60%). These animals were divided in three groups regarding M3 treatment: $M3_{HI}$ (n = 10) for a high dose of

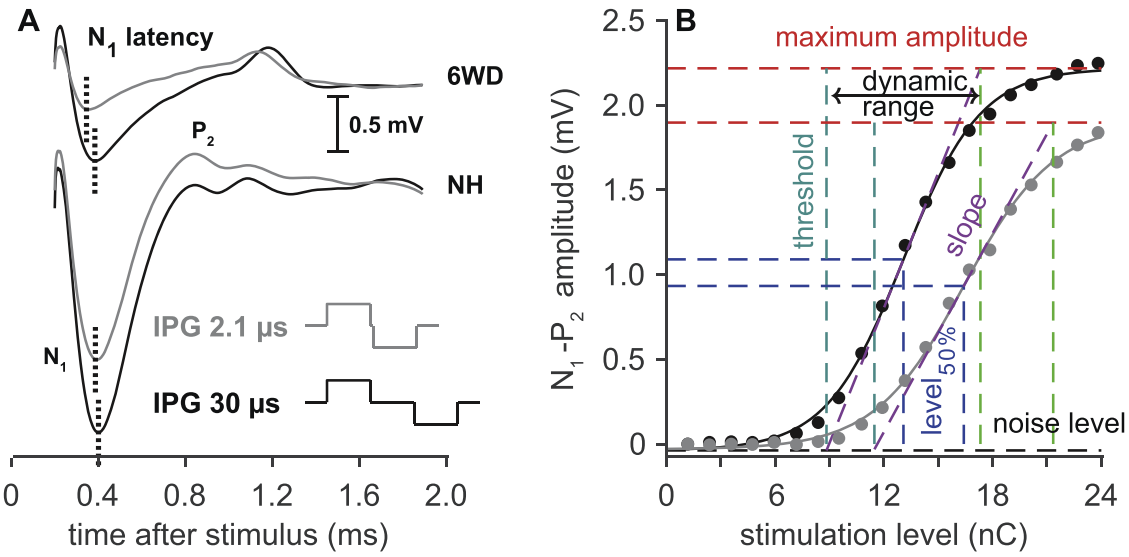

Fig. 2. Adapted from Vink et al., (2022) (their Fig. 1). (A) Two examples of eCAP recordings with different IPGs (30 µs: black line; 2.1 µs: grey line). The upper pair of recordings is from a 6 weeks deaf untreated control animal while the lower pair was recorded from a normal-hearing control animal. It is clear that the amplitude of the eCAP substantially decreases with deafness. Additionally, varying the IPG affects the properties of the eCAP. For instance, increasing the IPG to 30 µs increases the maximum amplitude and the N1 latency. (B) Input-output functions from N_1-P_2 amplitude in the same NH animal of A both an IPG of 2.1 µm (grey) and 30 µs (black). The line represents the Boltzmann curve fit. The dashed, colored lines represent the various eCAP characteristics. IPG: inter-phase gap.

M3, M3LO (n = 11) for a low dose of M3, and M3NO (n = 10) as control (see specifics in 2.2.2). After a brief acclimation period (1-2 weeks), all animals were bilaterally ototoxically deafened. For a schematic overview of the experimental timeline, see Fig. 1. Immediately prior, and two weeks after deafening click-evoked auditory brain stem responses (ABR) were recorded to assess the acoustic hearing thresholds. The right cochlea was then exposed by performing a bullostomy utilizing a retro-auricular approach. The round-window membrane (RWM) was punctured and covered with a small piece of gelatin sponge soaked with the treatment solution. Each animal's left cochlea was used as untreated internal (negative) control. Four weeks after treatment onset, the bullostomy was reopened and via a cochleostomy a custom-made electrode array (MED-EL, Innsbruck, Austria) was inserted into the scala tympani. The electrode array was connected to a MED-EL PULSAR CI stimulator, controlled by a PC running MATLAB via a RIB2 interface (Department of Ion Physics and Applied Physics, University of Innsbruck, Innsbruck, Austria). Extensive electrophysiological recordings were performed for several hours, after which the animals were terminated. The cochleas were subsequently harvested, fixed, decalcified and embedded in Spurr's low viscosity resin, after which cutting and sectioning was done of the cochlear regions of interest. In addition to the animals mentioned above, data from normal-hearing guinea pigs (NH, $n = 9$; obtained from Vink et al., 2020) and guinea pigs with a deafness duration of two weeks (2WD, $n = 5$; obtained from Ramekers et al., 2014) were included as reference data. Data from these animals were not included in the statistical analyses. This experiment was blinded, with the treatment solution unknown to the experimenters. Both SGC and eCAP data were analyzed prior to unblinding. All surgical and experimental procedures were approved by the Dutch Central Authority for Scientific Procedures on Animals (CCD: 1150020174315).

2.2. Surgical procedures

2.2.1. Deafening

Ototoxic deafening was performed following the same procedure as described in Vink et al. (2020, 2022). In short, following anesthesia, ABR recording was performed to confirm normal hearing (<40 dB SPL). Following this confirmation, kanamycin (400 mg/kg) was subcutaneously injected, followed by a single intravenous administration of furosemide (100 mg/kg).

2.2.2. M3 delivery

Two weeks after deafening, the animals received the treatment solution by gelatin-sponge-mediated delivery. This method has been described in detail by Vink et al. (2020, 2022). To summarize, the animals were anesthetized followed by ABR recording to confirm sufficient deafening as defined by a threshold shift of >50 dB. The right bulla was exposed by means of a retro-auricular incision, through which a small hole was made to expose the cochlea. Through this hole, the RWM of the cochlea was perforated and a small gelatin sponge (~1 mm^3) loaded with the treatment solution was placed hereon. This treatment solution consisted of one of three solutions, two of which containing monoclonal antibody M3 (Otonomy Inc., San Diego, CA, USA) in a histidine/arginine buffer: M3HI (n = 10), 3 µl of 7 mg/ml M3 [47 µM] in buffer; M3LO (n = 11), 3 µl of 0.7 mg/ml M3 [4.7 µM] in buffer; or M3NO (n = 10), 3 µl buffer.

2.2.3. Cochlear implantation

Four weeks after M3 delivery, animals received a custom-made electrode array in their treated right ear, the procedure of which has been described in detail by Vink et al. (2020, 2022). In short, after anesthesia, two transcranial screws were placed on the skull roughly 1 cm lateral of bregma, serving as a ground and reference electrode for the eCAP recordings. A tracheotomy was subsequently performed to artificially ventilate the animal throughout the remainder of the experiment. The bulla was re-exposed and reopened to allow access to the cochlea. A small (0.5 mm) cochleostomy was hand-drilled into the base of the cochlea, within 1 mm of the RWM, through which a ~0.45-mm-diameter electrode array was inserted up to approximately 4-5 mm, corresponding to location B2. The array containing four stimulation/recording contacts was then connected to the MED-EL PULSAR CI stimulator (MED-EL GmbH, Innsbruck, Austria). The most apical electrode contact was used for stimulation; one of the basal two contacts was used for eCAP recording.

2.3. Auditory brainstem response recordings

Click-evoked ABRs were recorded using three subcutaneous needle

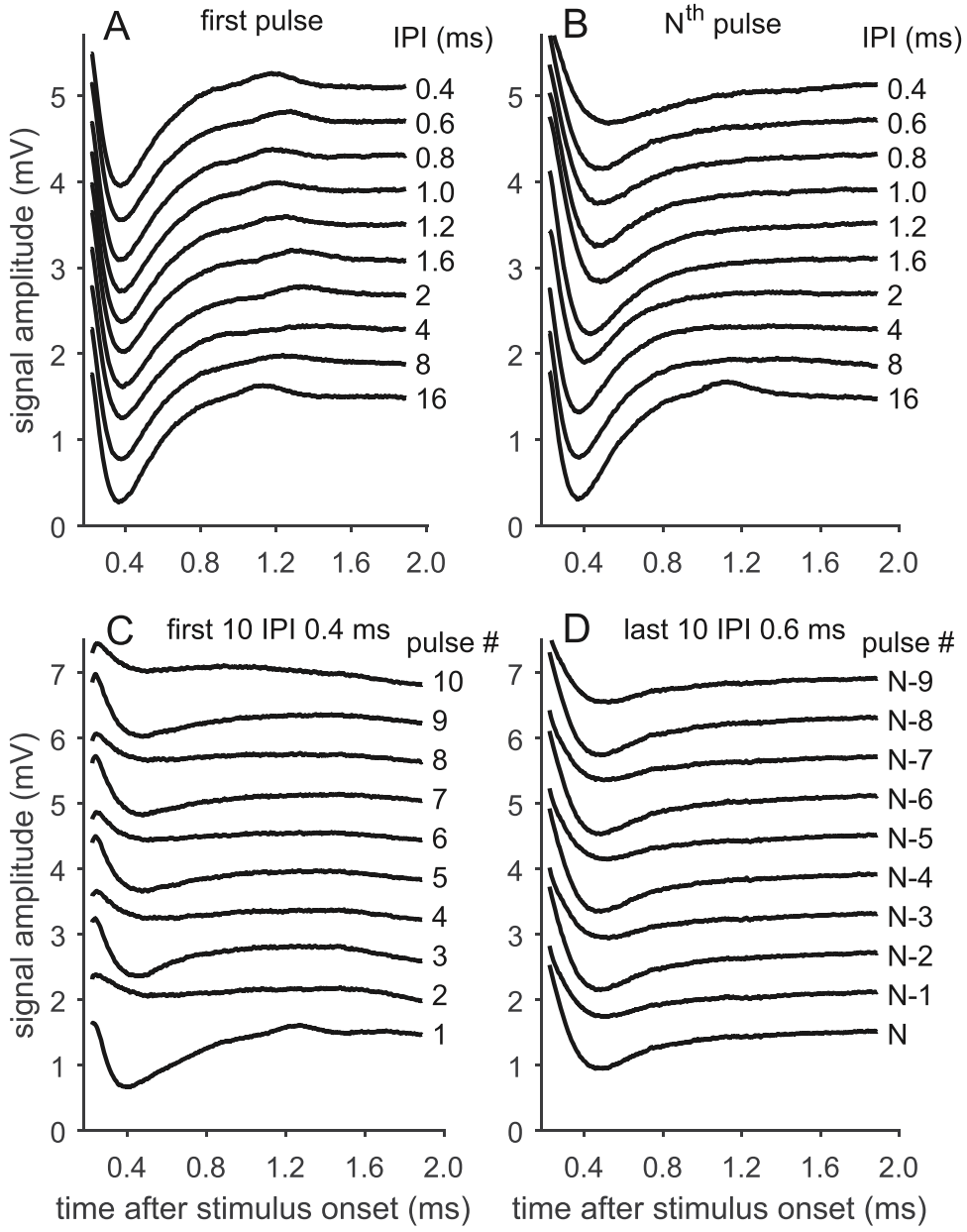

Fig. 3. Examples of eCAPs in response to pulse train stimulus. (A) The initial pulse of a pulse train logically evokes a highly similar eCAP, regardless of pulse rate. (B) The last pulse still evokes a similar response in case of the longest IPI of 16 ms, but the eCAP amplitude clearly decreases for shorter IPIs. The bottom row plots illustrate the alternating pattern that emerges for short IPIs (see text). (C) This pattern emerges instantaneously. (D) Especially in animals with low neural survival, this pattern can stabilize and remain present for the entire 100-ms duration of the pulse train. N^{th} pulse: the last pulse of the 100-ms pulse train.

electrodes: the active electrode was placed behind the right ear, the reference electrode was placed on the skull and the ground electrode was placed in the hind limb. A speaker (PCxb352; 4 Ω; 30 W, Blaupunkt (International) GmbH & Co. KG, Hildesheim, Germany) set at 10 cm distance from the right ear was used to present acoustic clicks (20 μs monophasic rectangular pulses; inter-stimulus interval 99 ms) synthesized and attenuated by a TDT3 system (Multi-I/O processor RZ6; Tucker-Davis Technologies, Alachua, FL, USA). The sound levels were calibrated by a sound level meter (Brüel & Kjaer, 2203) and a 1" condenser microphone (Brüel & Kjaer, 4132). The recordings were amplified using a Princeton Applied Research (Oak Ridge, TN, USA) 5113 pre-amplifier (× 5000; band pass filter 0.1–10 kHz) and digitized by the TDT3 system (100 kHz sampling rate, 24-bit sigma-delta converter) and stored for offline analysis. Hearing thresholds were determined by presenting a sound level of 110 dB peak equivalent SPL, which was decreased in steps of 10 dB until no response was observed. The threshold was defined as the interpolated sound level at which the ABR N1-P2 peak was 0.3 μV.

2.4. eCAP recordings

2.4.1. Single-pulse eCAP paradigm

Electric stimuli (biphasic current pulses of 30 μs/phase) were presented with alternating polarity to reduce stimulation artefact, and the responses to 50 pairs of these stimuli were averaged as described in Ramekers et al. (2014). The IPG of the stimuli was either 2.1 or 30 μs. Varying this IPG leads to differences in the eCAP, as illustrated in Fig. 2A. These differences, the so-called IPG effect (ΔIPG), have been shown to reflect neural health (Prado-Guitierrez et al., 2006; Ramekers et al., 2014, 2015a, 2022).

For both IPGs the stimulus pulse was presented at 20 charge levels, typically ranging from 1.2 to 24 nC; maximum charge level in all

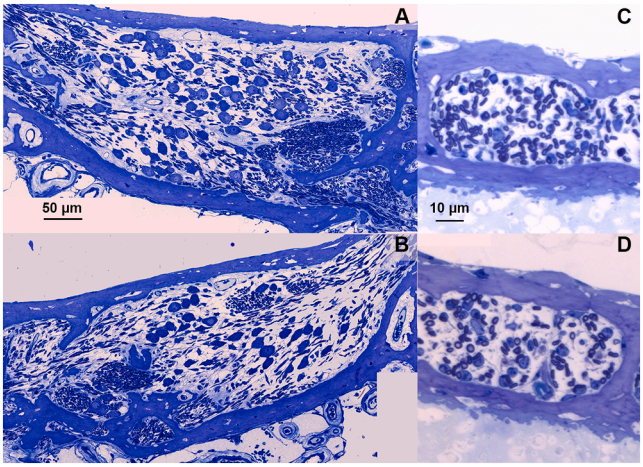

Fig. 4. (A,B) Examples of the B1 region of an M3HI-treated animal (19VIN20). (A) The treated ear (SGC packing density: 862 cells/mm^2). (B) The untreated ear (SGC packing density: 442 cells/mm^2). There is clear SGC degeneration in both images (compared to an average of 1412 cells/ mm^2 in normal-hearing animals), but more cells remain in the treated than the untreated B1 region. (C,D) Examples of PPs in the osseous spiral lamina, of the B region of an M3HI-treated animal (19VIN20). (C) The treated ear (PP packing density: 51 PPs/1000 μm^2) (D) The untreated ear (PP packing density: 38 PPs/1000 μm^2). As with the SGCs, clear loss of PPs can be observed in both images (compared to an average of 81 PPs/1000 μm^2), but there is a higher packing density of PPs in the treated ear at the B region.

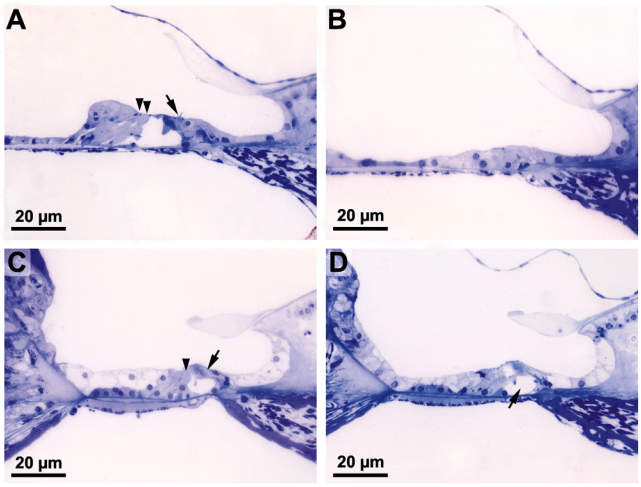

Fig. 5. Examples of light microscopical images of the organ of Corti from four different animals. The images in the top row exemplify unambiguous hair cell presence or absence; the examples in the bottom row indicate that hair cell identification in the progressively degenerating organ of Corti can be ambiguous. (A) Apical location A2 in an M3NO animal. The arrow indicates a clearly present inner hair cell with a nucleus and stereocilia; arrowheads point to two outer hair cells, meaning that the third outer hair cell is absent. (B) Middle location M2 in a M3NO animal, exhibiting a clearly advanced state of degeneration of the organ of Corti in which all hair cells are lost. (C) Basal location B1 in an M3LO animal. The organ of Corti is partially collapsed, but the inner (arrow) and one outer hair cell (arrowhead) are still present. (D) Basal location B1 in a M3LO animal. Some structures in the organ of Corti, such as the tunnel of Corti (arrow), are discernible; hair cells have died.

animals ranged from 24 to 27 nC (24 nC: n = 26; 25.5 nC: n = 5; 27 nC: n = 1). The eCAP amplitude – defined as the voltage difference between the N_1 and P_2 peaks (Fig. 2A) – was plotted against charge level, resulting in an input-output curve. Boltzmann sigmoid fitting was applied to this curve (Ramekers et al., 2014; Vink et al., 2020). Five measures were derived from this fit: the maximum amplitude, slope of the fit, threshold, dynamic range and the stimulation level corresponding to the half-maximum amplitude ($level_{50\%}$), shown in Fig. 2B. The sixth measure was the N1 latency derived from the eCAP waveform (Fig. 2A), averaged over the highest 3 current levels.

2.4.2. *Pulse-train paradigm*

The stimulus used for this assessment was a fixed-duration 100-ms pulse train with variable inter-pulse interval (IPI), described in detail in Vink et al. (2022). In short, these trains consisted of identical biphasic stimuli with a phase duration and IPG of 30 μs. The IPIs ranged from 0.4 to 16 ms, chosen such that the longest IPI did not cause any refractoriness or adaptation (i.e., every consecutive pulse evokes a similarly large response), while the smallest IPI was near the absolute refractory period (~0.4 ms) thus resulting in a transient disappearance of the eCAP (Fig. 3A,B). We recorded the response to the first 10 and those to the last 10 pulses of the 100-ms pulse train in stepwise fashion. Hence, we could capture both the initial rapid effects of neural refractoriness, and the adapted steady-state responses at the end of the stimulation.

An alternating pattern emerges at short IPIs (< 1 ms), in which odd-numbered pulses systematically evoke larger eCAPs than even-numbered pulses (Fig. 3C,D). The alternating pattern is quantified as amplitude modulation depth relative to the maximum eCAP amplitude, or 'modulation depth' in short. As this pattern for the first ten pulses (Fig. 3C) reliably emerges from the 5th pulse onward, the modulation depth of the pattern in response to the last 6 of the first ten pulses was determined. For the last ten pulses (Fig. 3D), the alternating pattern is consistently shown. As such, the modulation depth over all ten pulses was determined.

We have previously shown that the magnitude of the modulation depth is negatively correlated with neural survival (Ramekers et al., 2015a,b). This measure can therefore be used as an indicator of neural survival after neurotrophic treatment. To supplement these data, the eCAP N_1 latency at short IPIs was assessed, as this was shown to correlate strongly with SGC survival (Ramekers et al., 2015b; Vink et al., 2020). With decreasing IPI, N_1 latency increases (as seen in Fig. 3B). As for the modulation depth, for the analysis of the responses to the first 10 pulses, the mean N_1 latency was established for the last six of the first ten pulses. For the analysis of the responses to the last 10 pulses, the latency was averaged over all 10 pulses.

2.5. *Histological processing*

After fixing and embedding of the cochleas, semi-thin midmodiolar sections (1 μm thick) were cut. Two sections were selected (1 μm thick), at 30-μm intervals (or larger) to ensure consecutive sections would not contain the same cell. The sections were then stained using 1% methylene blue, 1% azur B and 1% borax in distilled water. Cross-sections of Rosenthal's canal (as exemplified in Fig. 4A,B) for six cochlear locations (B1, B2, M1, M2, A1 and A2) were photographed using a Leica DC450F digital camera mounted on a Leica DMRA light microscope and a 40 × oil immersion lens (Leica Microsystems GmbH, Wetzlar, Germany). SGCs were manually quantified in two of these midmodiolar sections with the image processing software ImageJ (version 1.52a). SGC packing density (cells/mm^2; see Van Loon et al., 2013 for a detailed description) was defined by the number of surviving SGCs within the surface area of the cross-section of Rosenthal's canal.

For PP quantification, cross-sections of the osseous spiral lamina were made perpendicular to the Rosenthal's canal cross-section, which allows the analysis of myelinated PPs (as exemplified in Fig. 4C,D) just before they exit the habenula perforata toward the organ of Corti. These cross-sections were made between the B1 and B2 cross-sections of their respective Rosenthal's canal in the basal turn, between M1 and M2 for the middle turn, and between A1 and A2 for the apical turn. As such the analyzed regions do not fully correspond to the six sections used for SGC quantification and will be reported as B, M and A for the basal, middle

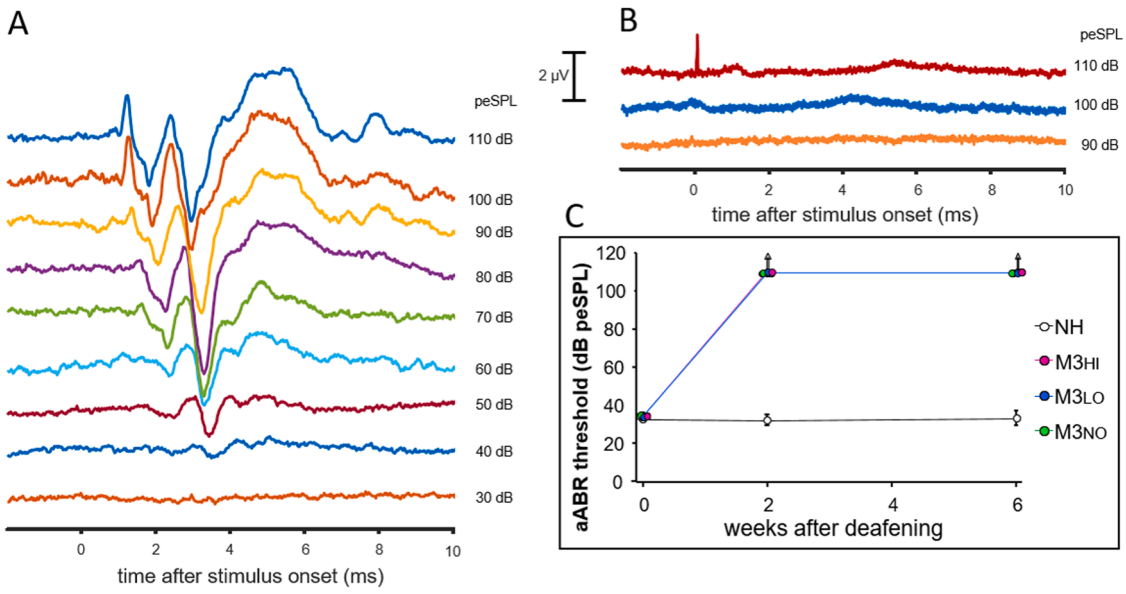

Fig. 6. Click-evoked auditory brainstem response (ABR) recordings. (A) Example of ABR recordings of an animal before deafening. (B) Example of ABR recordings of the same animal as in A, but and after deafening (M3HI group). The sound attenuation level to each recording is marked in dB with 0 dB corresponding to 110 dB peSPL. (C) Mean ABR thresholds for the different treatment groups as a function of time after deafening. The first ABR was recorded prior to deafening; note the similar threshold in all experimental groups. The second and third recordings were performed 2 and 6 weeks after deafening, respectively. Without exception, all deafened animals had a large threshold (minimal shift: 62 dB; well beyond the 50-dB criterion for successful induction of deafness), indicating severe to profound hearing loss. The arrows indicate that the threshold could not be attained even with the loudest possible stimulus in our set-up (110 dB peak equivalent SPL). NH: normal-hearing animals, $n = 9$; M3HI, $n = 10$; M3LO, $n = 11$; M3NO, $n = 10$ animals.

and apical turn, respectively. The sections for PP analysis were photographed with a 63 × oil immersion lens. PPs were subsequently quantified as the number of fibers in a given cross-sectional area of the osseous spiral lamina (PPs/1000 µm^2; see Ramekers et al., 2020).

The SGC and PP data have been normalized to corresponding data from normal-hearing animals (n = 27) obtained from previous studies (Ramekers et al., 2014, 2015a, 2020; Vink et al., 2020). The main outcome measure for both SGCs and PP is the packing density ratio between the treated ear (right ear; *auris dexter*, AD) and the contralateral ear (left ear; *auris sinister*, AS) as the effect of the different doses of M3 in comparison to the negative control.

Hair cell counts were performed in single midmodiolar sections of the organ of Corti at the 7 locations B1 – A3. Criteria were presence of a cuticular plate with cilia bundle, and a nucleus or a hair-cell-like outline at the expected location (Tisi et al., 2022). Histological examples of hair cells in our guinea pig modal of deafness are shown in Fig. 5.

2.6. Statistical analyses

The histological data were analyzed with a linear mixed model (LMM), under the assumption of compound symmetry using cochlear location, in relative distance to B1 (previously described in Van Loon et al., 2013), as a covariate and group as a factor. Independent *t*-tests were performed on a subset of data as descriptive *post hoc* analyses in order to support visual inspection of Figures.

For the single-pulse and eCAP and pulse train stimulation recordings, one-way analysis of variance (ANOVA) was performed to reveal any differences between the M3 groups, followed by *post hoc* testing with Tukey's HSD. Note that we did not test differences between M3 groups and NH or 2WD groups; differences in eCAP outcomes between 6 weeks deaf animals (as M3NO) and NH and 2WD have been demonstrated to be highly significant (Ramekers et al., 2014, 2022). In case the homogeneity of variances assumption was violated, a Kruskal-Wallis analysis of variances was performed. Additionally, for the pulse train data, a linear regression analysis was used to elucidate the relationship between the pulse-train outcome measures and corresponding histological data.

3. Results

3.1. Deafening

An example of ABRs of a normal-hearing animal is shown in Fig. 6A. The ABR recording two weeks after deafening in the same animal was performed to assess the extent of hearing loss (Fig. 6B). All animals were considered sufficiently deafened, as the minimal recorded threshold shift of 62 dB exceeded the 50-dB inclusion criterion (Fig. 5C).

Along with the large ABR threshold shifts, we found a substantial loss of cochlear hair cells, as counted in a single midmodiolar cochlear section for each animal. The survival of the hair cells (Fig. 7A) was normalized to the presence of hair cells in normal-hearing animals (i.e. 100%). In all three experimental groups, there was severe loss of both inner and outer hair cells, which did not differ between the treated and the untreated ears in either of the three experimental groups (paired *t*-test, IHC:, $p_{M3LO} = 0.59$, $p_{M3NO} = 0.12$; OHC: $p_{M3HI} = 0.29$, $p_{M3LO} = 0.052$, $p_{M3NO} = 0.47$). In the M3HI group the data was not normally distributed for the inner hair cells; therefore the Wilcoxon Signed-Ranks Test was applied, which revealed no difference between the treated and untreated ears ($p_{M3HI} = 0.93$). Although there was hair cell survival, the absence of an ABR (Fig. 6B) indicates that these surviving hair cells are unlikely to have been functional.

3.2. Auditory nerve histology

Examples of SGC packing density in B1, and PP packing density in B, for both the treated and untreated ear of the same M3HI-animal are shown in Fig. 4. In both cochleas, substantial SGC and PP degeneration has taken place, but importantly there are more SGCs and PPs present in the treated than in the untreated ear.

3.2.1. Spiral ganglion cells

Fig. 8A–C shows SGC packing density, normalized to the mean SGC packing densities in normal-hearing control animals for each cochlear location separately. For some animals (M3HI, $n = 1$; M3LO, $n = 1$; and

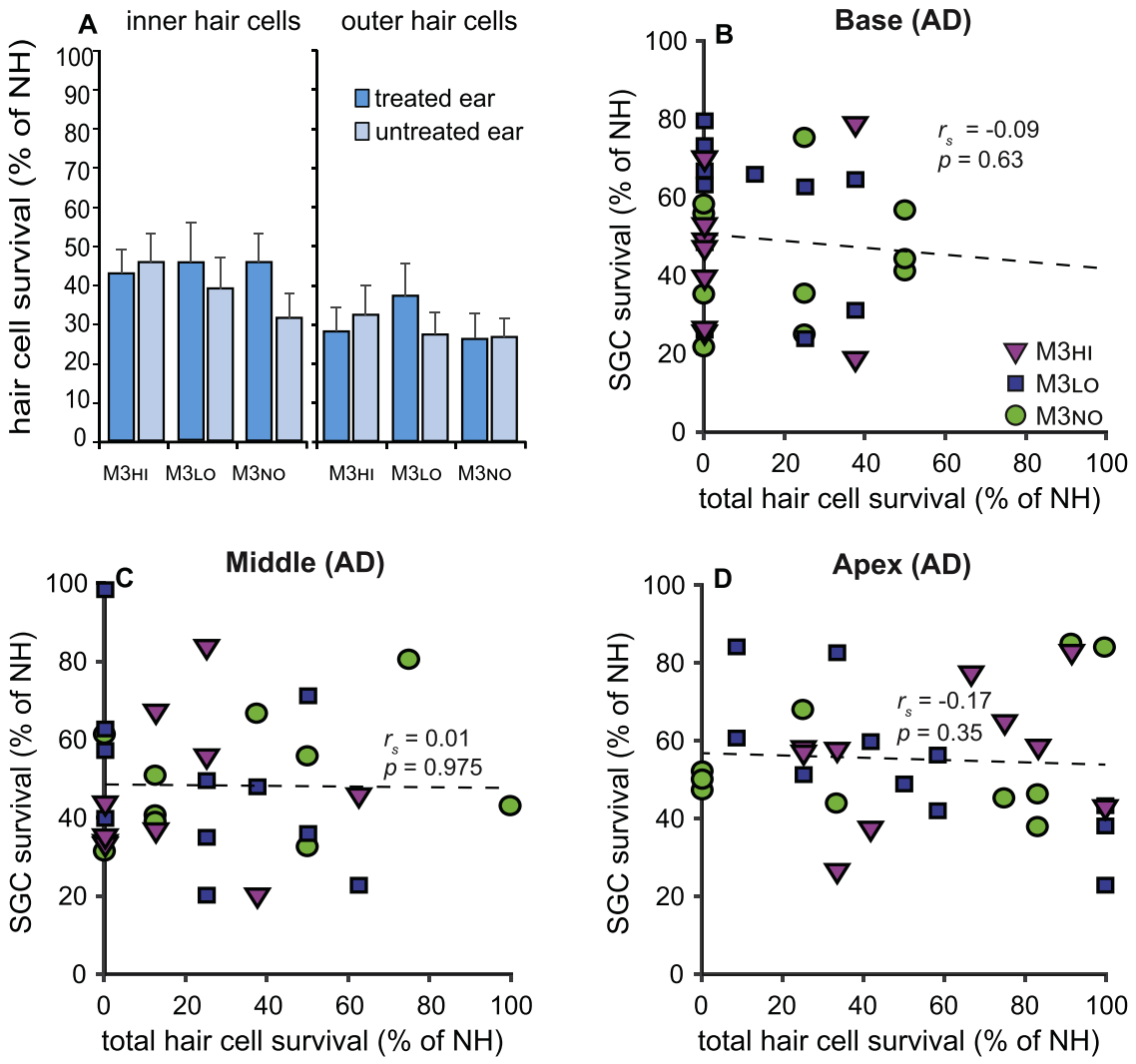

Fig. 7. Hair cell survival. Percentage of survival as compared to the normal-hearing situation for the inner hair cells (left) and outer hair cells (right) for the three M3 treatment groups. To assess differences between the treated and untreated ears, paired *t*-tests were performed; no significant differences were found. Error bars represent SEM. M3HI, $n = 10$; M3LO, $n = 11$; M3NO, $n = 10$ animals. (B) Normalized SGC survival versus normalized hair cell survival for the basal turn of the treated right cochlea. Counts of lower and upper basal turn have been averaged. Counts of inner and outer hair cells have been summed. Spearman's rank correlation analysis has been performed. (C) As B for middle turn. (D) As B for apical turn.

M3NO, $n = 2$) no SGC quantification was possible for the B1 region in either the treated or contralateral ear; this was either because of a damaged region (no reliable quantification), or because the region was absent from the microscopic section due the angle along which the cochlea was cut. For both the high (M3HI, Fig. 8A) and low M3 dose (M3LO, Fig. 8B) the group means of the treated ear were consistently higher than or similar to the contralateral ear across the cochlea. In particular at the B1 region there was more SGC survival in the right ear than the untreated left ear. In the control group M3NO (Fig. 8C), such an effect was absent, as the contralateral ear showed for most locations very similar cell survival. To assess the differences between the treated ear (AD) and the untreated ear (AS) the Log_2 transformed AD/AS ratio of the SGC packing density was calculated for each individual animal before averaging (shown in Fig. 8D). With this transformation, positive values indicate more SGC survival in the treated ear, and negative values indicate more SGC survival in the untreated ear. This Figure shows that the mean SGC survival ratio in both M3-treated groups was positive in nearly all cochlear locations, predominantly in the lower basal turn of the cochlea, except in M1 for M3LO and A2 for both treatment groups. A linear mixed model on the Log_2 transformed AD/AS ratio revealed a significant M3 treatment effect ($F_{(2,83.9)} = 4.0$; $p = 0.021$), with more SGC survival in both the M3HI ($t_{(81.1)} = 2.0$; $p = 0.050$) and M3LO ($t_{(81.1)} = 2.7$; $p = 0.007$), than in the M3NO group. No interaction effect was found between treatment and cochlear location ($F_{(2,80.1)} = 1.7$; $p = 0.18$).

We further examined SGC survival for all cochlear locations in which the mean log ratio of the M3HI and M3LO groups exceeded that of the M3NO group, to see in which cochlear location a significant treatment effect was observed.

For the M3HI group, the enhanced SGC survival was significant in the lower basal turn (untransformed AD/AS ratio: 1.37; one-tailed independent t-test; $t_{B1(15)} = 1.8$, $p = 0.049$) and in the lower apical turn (untransformed AD/AS ratio: 1.31; $t_{A1(18)} = 2.2$, $p = 0.021$). For the M3LO group there was significantly higher SGC survival than the M3NO group in both the lower and upper basal turns, as well as the upper middle turn (one-tailed independent t-test; $t_{B1(16)} = 2.0$, $p = 0.029$; $t_{B2(15,6)} = 2.6$, $p = 0.020$; $t_{M2(14.8)} = 2.7$, $p = 0.0081$; untransformed AD/AS ratios: B1: 1.46; B2: 1.21; M2: 1.23).

Differences in SGC survival between the three groups may be related to incidental differences in hair cell survival. Particularly interesting is the enhanced SGC survival in middle and apical turns. Therefore, we examined the relation between SGC and hair cell survival for basal,

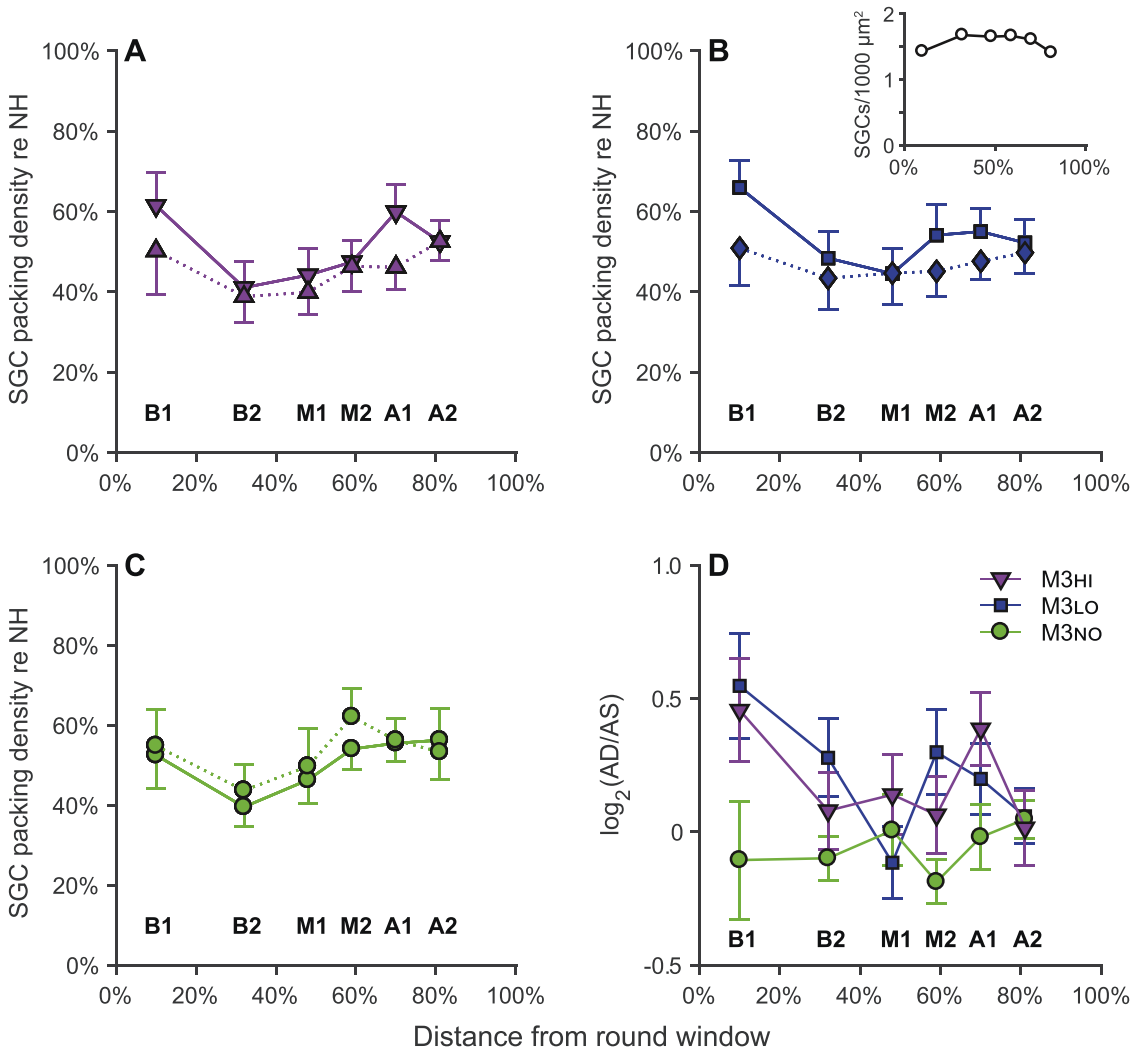

Fig. 8. Normalized SGC packing density as a function of cochlear location in relative distance from the round window, where 0% is round window and 100% is the helicotrema. (A) Group means of M3HI, downward triangle with solid line represents the treated ear (AD), upward triangle with dotted line represents the contralateral ear (AS). (B) Group means of M3LO, square with solid line represents the treated ear (AD), diamond with dotted line represents the contralateral ear (AS). (C) Group means of M3NO, circle with solid line represents the treated ear (AD), circle with dotted line represents the contralateral ear (AS). (D) Log transformed AD/AS ratio of the SGC packing density for all three groups. Note that the log transformed AD/AS ratio was calculated for each individual animal and subsequently averaged, therefore it deviates from the Log_2 of the ratio of the averages shown in A-C. The inset in A represents the mean SGC packing density of normal-hearing animals, as a reference. M3HI, $n = 10$ ($n = 9$ for B1); M3LO, $n = 11$ ($n = 10$ for B1); M3NO, $n = 10$ animals ($n = 8$ for B1). B1 to A2 represent cochlear locations from base to apex. Error bars represent SEM.

middle and apical turn separately. For the treated right ears there was no correlation between SGC and hair cell survival in either cochlear location ($p > 0.3$) as depicted in Fig.7B–D. SGC survival was not correlated to hair cell presence in the left cochleas either ($p > 0.1$).

3.2.2. *Peripheral processes*

In Fig. 9A–C, the PP packing density was normalized to the mean PP packing densities in normal-hearing control animals for the basal (B), middle (M) and apical (A) turns. The highest PP survival can be seen in the M3HI group (Fig. 9A). For the M3LO group (Fig. 9B), the treatment effect appeared to be limited to the basal and middle turns. As with the SGCs, the Log_2 transformed AD/AS ratio was calculated to investigate the difference between the treated and contralateral ear (Fig. 9D). A linear mixed model on the transformed AD/AS ratio did not reveal an M3 treatment effect ($F_{(2,32.5)} = 1.3$, $p = 0.29$) over the entire cochlea, nor an interaction effect between treatment and cochlear location ($F_{(2,57.4)} = 0.5$, $p = 0.60$). As with the SGCs, Fig. 9D shows possible treatment effects in certain cochlear locations, since the mean ratio of treated groups exceeded that of the untreated group in the basal and apical turns (M3HI only). In turn, we further examined these locations.

A one-tailed independent *t*-test revealed significantly higher PP survival in the M3HI group than the M3NO group for the basal turn (untransformed AD/AS ratio: 1.52; one-tailed independent t-test; $t_{B(18)} = 1.9$, $p = 0.038$). No significantly higher PP survival was observed in the basal turn for the M3LO group as compared to the M3NO group (untransformed AD/AS ratio: 1.27; one-tailed independent t-test; $t_{B(19)} = 0.6$, $p = 0.27$).

3.2.3. *PP versus SGC preservation*

In Fig. 10 the normalized PP survival is shown as a function of normalized SGC survival across the entire cochlea for the treated ear (Fig. 10A) and the untreated ear (Fig. 10B). The black diagonal line indicates a 1:1 ratio of PP/SGC presence. Closeness to this line means that both SGCs and PPs were equally well preserved. Concordantly, the more distance from this line, the more survival is skewed in favor of either PPs (points above the line) or SGCs (points below the line). Looking at the treated ear (Fig. 10A) the majority of all animals, regardless of treatment group, were located near the diagonal, albeit

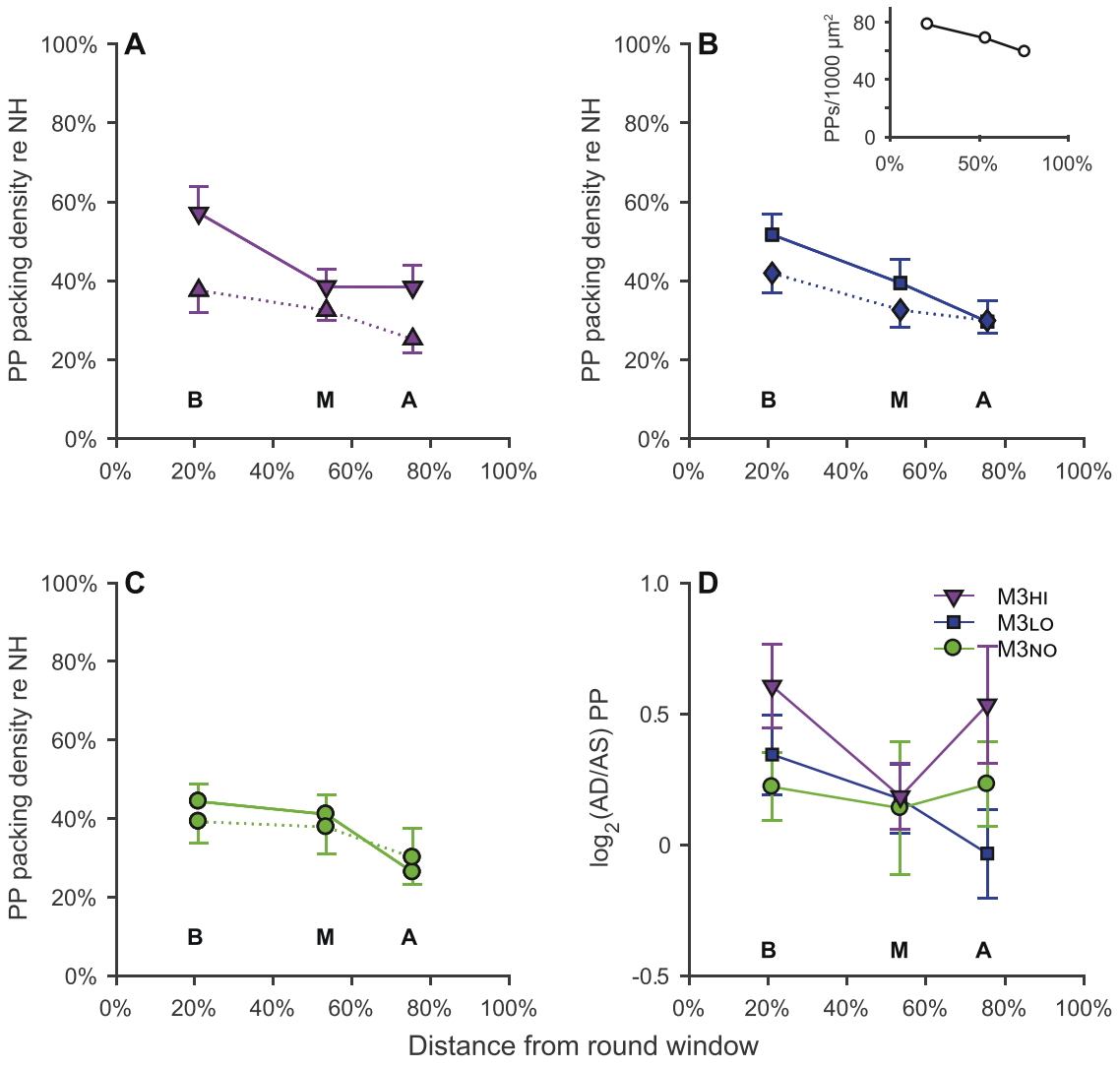

Fig. 9. Normalized PP packing density as a function of cochlear location in relative distance from the round window, where 0% is round window and 100% is the helicotrema. (A) Group means of M3HI, downward triangle with solid line represents the treated ear (AD), upward triangle with dotted line represents the contralateral ear (AS). (B) Group means of M3LO, square with solid line represents the treated ear (AD), diamond with dotted line represents the contralateral ear (AS). C) Group means of M3NO, circle with solid line represents the treated ear (AD), circle with dotted line represents the contralateral ear (AS). D) Log transformed AD/AS ratio of the PP packing density for all three groups. Note that the log transformed AD/AS ratio was calculated for each individual animal and subsequently averaged, therefore it deviates from the Log_2 of the ratio of the averages shown in A-C. The inset in A represents the mean PP packing density of normal hearing animals, as a reference. M3HI, $n = 10$ ($n = 9$ for A); M3LO, $n = 11$ ($n = 10$ for A); M3NO, $n = 10$ animals ($n = 8$ for M and (A). B, M, and A represent cochlear locations from base to apex. Error bars represent SEM.

mainly below the line, with the ratios of the different groups: M3HI = 0.91, M3LO = 0.79 and M3NO = 0.78. This indicates less PP than SGC preservation. Indeed, the PP/SGC ratio of all three groups were significantly lower than 1 (one-sided one-sample *t*-test, M3HI: $t_{(9)} = 2.1$, $p = 0.030$; M3LO: $t_{(10)} = 5.8$, $p < 0.001$; M3NO: $t_{(9)} = 5.1$, $p < 0.001$). Note that the PP/SGC ratio for treated animals did not substantially differ with that for untreated M3NO animals (one-way ANOVA, $F_{(2,28)} = 3.2$, $p = 0.058$). In the untreated contralateral ear (Fig. 10B) the PP/SGC ratio of all experimental groups are situated below the 1:1 line, which indicates a larger presence of SGC soma than their PPs. As with the treated ear, no differences were observed between the experimental groups (one-way ANOVA, $F_{(2,28)} = 0.23$, $p = 0.58$). The PP/SGC ratios considered for each location separately (basal, middle, apical) appeared close to 1 for the basal and relatively low for the apical location (not shown).

3.3. Electrophysiological results

3.3.1. Single pulse recordings

Fig. 11 presents group averages of the six eCAP characteristics obtained with a 2.1-µs IPG stimulus (left column), a 30-µs IPG stimulus (middle column), and the difference between these outcomes, the IPG effect (ΔIPG, right column). eCAP data from NH and 2WD animals have also been included for illustration purposes. These data were not included in the statistical analyses, since we are interested in the differences among the three experimental groups.

Neural degeneration affected the absolute characteristics; most prominently the maximum amplitude (Fig. 11A,B), slope (Fig. 11D,E) and latency (Fig. 11P,Q) decreased after deafening.

For only one of the six measures, the dynamic range (Fig. 11J-L), significant differences were found between treated and untreated groups. The dynamic range of the M3HI group was smaller than that of the M3NO group for an IPG of 30 µs (Fig. 11K), whereas the dynamic range of the M3LO group was significantly smaller at both IPGs than the

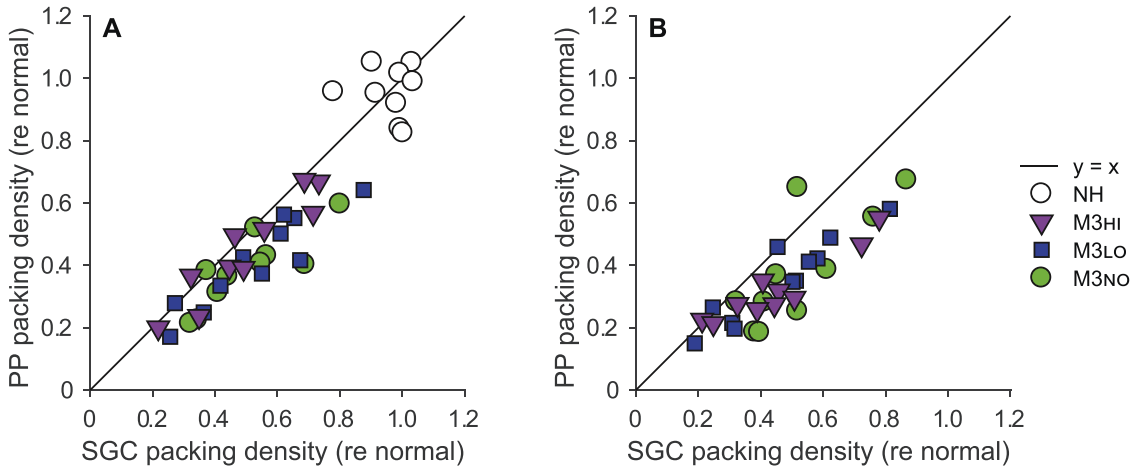

Fig. 10. Normalized PP packing density as a function of normalized SGC packing density averaged across all cochlear locations. (A) All individual animals of each M3 experimental group for the right treated ear and (B) the left untreated ear. Data from normal-hearing animals ($n = 9$) in A are included from Vink et al. (2020) which used the same methodology as the present study; normalization of the presented data was performed with data from 27 NH animals, as described in Section 2.4.

M3NO group (Fig. 11J,K), and no differences were observed between the M3HI and M3LO groups (one-way $ANOVA_{IPG\ 2.1\ \mu s}$, $F_{(2,27)} = 3.6$, $p = 0.040$; Tukey's HSD, $p_{(M3HI\text{-}M3NO)} = 0.17$; $p_{(M3LO\text{-}M3NO)} = 0.035$, $p_{(M3HI\text{-}M3LO)} = 0.72$; one-way $ANOVA_{IPG\ 30\ \mu s}$, $F_{(2,27)} = 4.4$, $p = 0.022$; Tukey's HSD, $p_{(M3HI\text{-}M3NO)} = 0.050$; $p_{(M3LO\text{-}M3NO)} = 0.030$; $p_{(M3HI\text{-}M3LO)} = 0.98$).

No statistically significant differences were observed when assessing the ΔIPG outcomes for any of the six eCAP measures. Nevertheless, the group means of the M3-treated groups generally gravitated more towards the ΔIPG effect data of normal-hearing animals than the M3NO group, which differed the most from the NH animals (most notably for latency). In addition, no statistically significant correlation between any of the ΔIPG measures and SGC packing density was observed for the experimental groups (data not shown).

3.3.2. *eCAP recordings to pulse train stimulation*

Two animals were excluded from the pulse-train analyses due to unreliable recordings, one from the M3HI group and one from the M3LO group.

Fig. 12 shows the results of last six of the ten first pulses (see section 2.3.2). The modulation depth (Fig. 12A) was highest at IPIs of 0.4 and 0.6 ms. The modulation depth to the latter IPI was subsequently analyzed further, as we have previously found a strong correlation between modulation depth and SGC packing density for this IPI (Ramekers et al., 2015a,b; Vink et al., 2020). No statistically significant difference was observed between the three groups at an IPI of 0.6 (one-way ANOVA; $F_{(2,28)} = 0.4$, $p = 0.70$). The modulation depth for each individual animal at an IPI of 0.6 ms is shown as a function of the averaged SGC survival across the entire cochlea in Fig. 12B. The modulation depth had a significant negative correlation ($R^2 = 0.38$, $p = 0.005$) with untreated control animals (NH and M3NO), showing a smaller modulation depth with high SGC survival. In both M3-treated groups, no correlation ($R^2 = 0.03$; $p = 0.47$) was observed between modulation depth and SGC survival.

The Δlatency (defined as the difference in N_1 latency between an IPI of 0.6 and 16 ms; see red dashed boxes in Fig. 12C) was highest in the NH animals. The group means of M3HI and M3NO overlapped, whereas the Δlatency in the M3LO was the highest of the three. This was, however, not statistically significant (Kruskal-Wallis, $H = 0.95$, asymptotic $p = 0.66$). The ΔN_1 latency, shown in Fig. 12D as a function of SGC survival, correlated significantly with the untreated animals ($R^2 = 0.60$, $p < 0.001$), with a longer ΔN_1 latency with increasing SGC survival. This relationship was not significant for the M3-treated animals ($R^2 = 0.02$, $p = 0.60$), as the animals that show the highest SGC survival, exhibited a similar Δlatency as those with lower SGC survival. Note that correlations mentioned above do not substantially change when considering specifically SGC survival in the basal turn, where the electrodes are located ($R^2 = 0.35$ versus 0.38 and R^2=0.63 versus 0.60).

At the end of the pulse train the modulation depth (Fig. 13A) has diminished at the short IPIs (≤2 ms) as compared to the first ten pulses (Fig. 12A). All three M3 groups were virtually indistinguishable, and indeed at an IPI of 0.6 ms no significant difference between the three was observed (one-way ANOVA; $F_{(2,28)} = 0.3$, $p = 0.74$). As with the first ten pulses, the modulation depth for the last ten pulses in the untreated groups correlated strongly and significantly with SGC survival (Fig. 13B, black line). Additionally the treated animals roughly follow this same pattern with a weak but significant correlation between modulation depth and SGC ($R^2 = 0.24$, $p = 0.03$).

At the end of the pulse train the N_1 latency (Fig. 13C) increased for all groups as compared with the first ten pulses (Fig. 12C), predominantly for the IPI below 4 ms. As with the first ten pulses, the M3LO group had the highest Δlatency of the three M3 groups, but not significantly so (one-way ANOVA; $F_{(2,28)} = 2.1$, $p = 0.15$).

There was a significant positive correlation between ΔN_1 latency and SGC survival (Fig. 13D) for the untreated groups ($R^2 = 0.65$, $p < 0.001$), but not the M3-treated groups ($R^2 = 0.03$, $p = 0.44$). As with the first ten pulses, the animals with high SGC survival showed roughly the same ΔN_1 and latency, regardless of group.

4. Discussion

In the present study we investigated the preservative effects of the TrkB selective monoclonal antibody agonist M3, previously observed *in vitro*, on the auditory nerve *in vivo* by means of gelatin-sponge-mediated delivery in the ototoxically deafened guinea pig. We expected (1) M3 to preserve the SGCs and their PPs following deafness, and (2) this structural preservation to be reflected in functional preservation. Structural preservation was observed mainly in the SGCs and to a lesser extent their PPs. No functional preservation could be determined.

4.1. *The effect of M3 on cellular preservation*

In line with our expectations, treatment with M3 resulted in significantly stronger preservation of SGCs and their PPs than the untreated control animals, consistently in the lower basal turn and occasionally in the upper middle and lower apical turn of the cochlea. We analyzed hair cell survival after ototoxic treatments to examine whether differences in

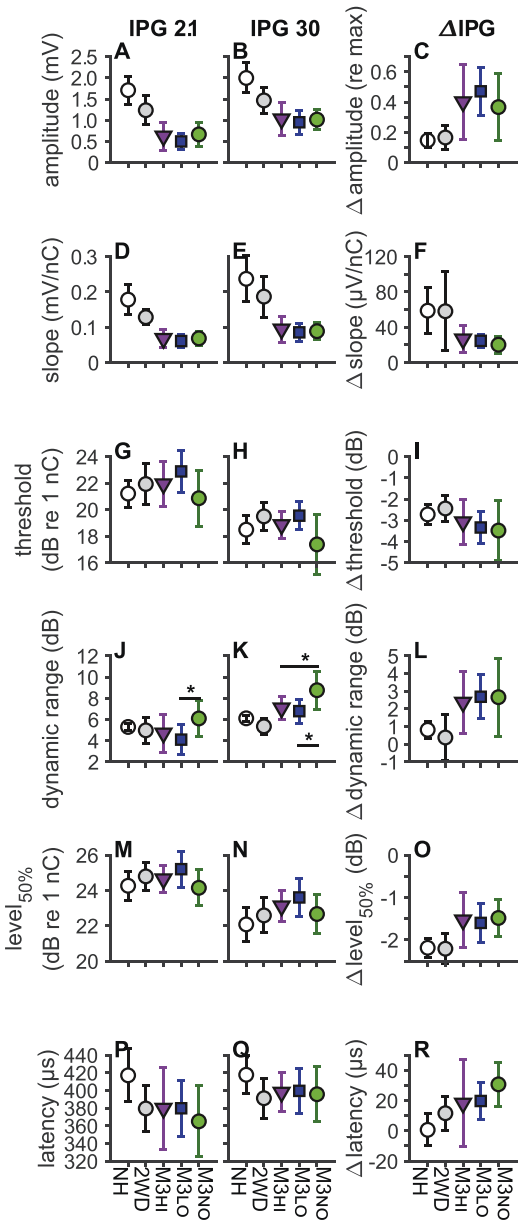

Fig. 11. Mean eCAP characteristics for each experimental group. The interphase gap (IPG) in the biphasic current pulse was 2.1 μs in the left column and 30 μs in the middle column. The difference between the two (i.e., the IPG effect) is shown in the third column. (A-C) maximum amplitude; D-F) slope; (G-I) threshold; (J-L) dynamic range; (M-O) $level_{50\%}$; (P-R) N1 latency. Good neural health is indicated by an IPG effect near NH values. One-way analyses of variance (ANOVAs) were performed to assess differences between the M3 treatment groups, followed by *post hoc* Tukey's HSD. No significant differences were revealed within the IPG-effect data. NH, $n = 9$; 2WD, $n = 5$ M3HI $n = 10$; M3LO, $n = 11$; M3NO, $n = 10$ animals ($n = 9$ for D, E, F, J, K, L).
*$p < 0.05$. Error bars represent SD.

SGC survival between the three experimental groups could be due to differences in hair cell survival. Since hair cell survival does not differ among the three experimental groups nor between M3-treated cochleas and contralateral cochleas, differences between SGC survival are unlikely to be caused by differences in HC survival.

In vitro, Szobota et al. (2019) observed a preservative effect of M3 very similar to that of BDNF, with a 10-fold lower dose of M3 (1 nM M3 versus 10 nM BDNF). In the present *in vivo* study, we used a 5-fold lower dose of M3 (47 μM) than BDNF used in a previous study (240 μM; Vink et al., 2020). As such, we expected to find SGC and/or PP preservation in the cochlea to be at least on the same level as that with BDNF. This was, however, not the case. Treatment with either M3HI or M3LO preserved a ratio of approximately 1.4 more SGCs in the lower basal turn (B1; Fig. 8D) of the treated relative to the untreated contralateral ear, and treatment with M3HI preserved 1.5 more PPs in the basal turn relative than in that of the untreated contralateral ear. In contrast, treatment with BDNF resulted in 2.1 more basal SGC and PP survival relative to the untreated contralateral cochlea (Vink et al., 2022). Beyond the basal turn, treatment with M3 yielded enhancement of survival at some locations (M3HI at A1: a ratio of 1.3; M3LO at M2: a ratio of 1.2). Such preservation beyond the basal regions was not observed in the deafened guinea pigs treated with either BDNF or NT-3 (Vink et al., 2022). This observation could, in part be due to the presumed higher biostability (i.e., longer half-life) of M3 as compared to BDNF or NT-3 (as proposed by Szobota et al. 2019), allowing for a longer time period for M3 to diffuse throughout the cochlea. Indeed, after intracochlear injection in the guinea pig, NT-3 is almost completely eliminated from the cochlea by 3 days and shows a marked base to apex gradient (Richardson et al., 2019). The pharmacokinetic properties of M3 are presumably better than those of BDNF in spite of its larger molecular weight (M3: 150 kDa vs BDNF: 27 kDa). The effect of M3 in the middle and apical locations may have been at the expense of the efficacy in the basal turn. Although no significant interaction between M3-mediated preservation and cochlear location was observed, the enhancement of survival appeared most convincingly in the basal turn, which may be ascribed to a TrkB expression gradient from base to apex (Schimmang et al., 2003). Another reason for the small effect of M3 may be a lack of virtuous cycle (also referred to as autocrine loop), which is proposed for BDNF (Canossa et al., 1997), explaining the long-term sustained neuroprotective effect of BDNF after cessation of exogenous delivery (Ramekers et al., 2012, 2015a). Possibly M3 does not induce BDNF synthesis because it does not co-activate p75NTR. It should also be noted that the degree to which M3 enters the cochlea in the present experiments is unknown and may be a contributing factor to the limited effect of M3. However, previous data in the rat indicate that M3 can achieve therapeutically-relevant levels in the cochlea after intratympanic administration in a poloxamer formulation (Tsivkovskaia et al., 2021), indicating that M3 can penetrate the round window membrane.

As the preservative effect was limited, but very similar for M3HI and M3LO, the dosages presented here are unlikely to be the optimal effective dose for M3 in this specific animal model. Based on the data presented here, it is not possible to determine the optimal dose of M3 *in vivo*.

An interesting histological observation was the unbalanced survival of SGCs and PPs. When averaged across the cochlea, less PPs than their SGCs were preserved in both the M3-treated groups and the untreated control group, and notably also the contralateral ears of all groups. In comparison, gelatin-sponge-mediated treatment with BDNF, NT-3, or a combination thereof has shown a PP/SGC ratio of >1 across the cochlea (Vink et al., 2022). However, poorer preservation of PPs than of SGCs following neurotrophic treatment is not unique. Similar results have previously been observed following BDNF treatment (Wise et al., 2005; Leake et al., 2011; Waaijer et al., 2013; Vink et al., 2021), with a PP/SGC ratio of <1 in the BDNF-treated ears and a PP/SGC ratio of ≥ 1 for the untreated ears, as discussed in Vink et al. (2021; their Fig. 8). This could indicate that PPs are more vulnerable than their SGCs, and will often degenerate despite of neurotrophic treatment. As such, treatment with M3 did not lead to the preservation of the PPs connected to each preserved SGC. It should however be considered that the observed SGC preservation was for a large part accounted for by the B1 region of the cochlea, without any apparent preservation in B2, whereas the preservation of PPs was quantified in the region in between B1 and B2. It is therefore entirely possible that the PP/SGC ratio presented in this study is an underestimation of the actual ratio at exactly the same location. It is important to note here that it is methodologically not possible to obtain OSL cross-sections containing PPs perpendicular to the exact same area of the corresponding Rosenthal's canal containing the SGCs,

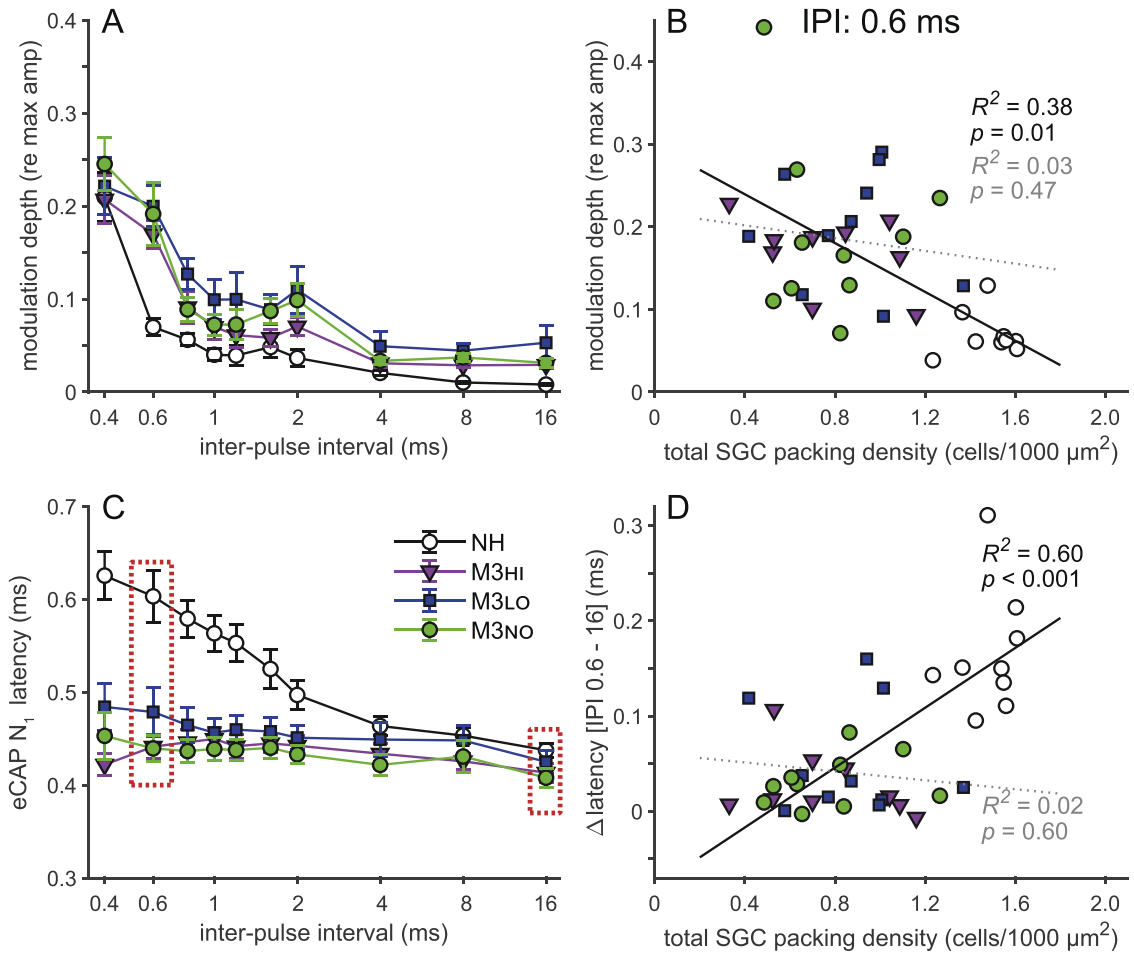

Fig. 12. Pulse train response parameters. (A) Group means of normalized modulation depth determined for the last 6 pulses of the first 10 pulses from the 100 ms pulse train as a function of IPI. (B) Group means of eCAP N_1 latency averaged over the last 6 pulses of the first pulses from the 100 ms pulse train as a function of IPI. (C) Modulation depth for 0.6-ms IPI for individual animals as a function of SGC packing density averaged across the entire cochlea. The black regression line and parameters are based on untreated (NH and M3NO) animals only, the dotted grey regression line and parameters are based on both treatment groups. (D) The difference in N_1 latency between 0.6-ms IPI and 16-ms IPI (dashed boxes in (B) as function of basal spiral ganglion cell packing density. The black egression line and parameters are based on untreated (NH and M3no) animals only, the dotted grey regression line and parameters are based on both treatment groups. NH, $n = 9$; M3HI, $n = 9$; M3LO, $n = 10$; M3NO, $n = 10$ animals. IPI, inter-pulse interval. Error bars represent SEM.

as the tissue from which the OSL cross-sections are obtained is lost in order to obtain the cross-sections of Rosenthal's canal, and vice versa (see Waaijer et al., 2013; their Fig. 1 for a schematic visualization).

For the untreated control group, the PP/SGC ratio of 0.78 was puzzling, considering the PP/SGC ratio of ~1 observed in the untreated control animals from a previous study using a similar methodology (Vink et al., 2022). The former observation is in line with the phenomenon 'retrograde degeneration', in which the PPs degenerate prior to their cell bodies, observed in different animals and humans (Spoendlin, 1975, 1985; Leake and Hradek, 1988; Shepherd and Javel, 1997). However, both SGCs and PPs are found to degenerate simultaneously in the presently used guinea pig model (Ramekers et al., 2020). Application of the vehicle solution cannot explain the discrepancy, since the contralateral ear showed a similarly low PP/SGC ratio (Fig. 10B).

4.2. Absence of functional preservation

With M3 resulting in significant preservation of both SGCs and PPs, we did expect this to be reflected in the functional measurements. This expectation is based on a study in which structural auditory nerve preservation following BDNF and/or NT-3 treatment *via* gelatin-sponge delivery showed a clear significant effect on the IPG effect measures, with the exception of eCAP latency (Vink et al., 2022). For the single-pulse eCAP recordings, the IPG effect had previously been shown to be a good indicator of neural health (Prado-Guitierrez et al., 2006; Ramekers et al., 2014, 2015a, 2022). However, the M3-mediated SGC and PP survival was not paired with any significant changes in the IPG effect as compared to the untreated control group. The eCAP measures were compared to SGC survival averaged across the entire cochlea (as opposed to for local cochlear regions) for following reasons. For most of the eCAP measures current levels were high and neurons in all regions are contributing to the eCAP, and averaging over more samples yields a more robust and reliable outcome (see further in Ramekers et al., 2022).

As CI functionality relies on high-frequency pulsatile stimulation delivered to the auditory nerve, we furthermore investigated whether a possible treatment effect could be observed in the pulse-train stimulation paradigm. However, for both the first 10 and the last 10 pulses of a 100-ms pulse train, no such effect could be observed.

At the end of the 100-ms series of pulses, a correlation was observed between neural survival in the M3-treatment groups and the modulation depth (Fig. 13B). A relationship which was not observed previously following gelatin sponge-mediated neurotrophin treatment (Vink et al., 2022). This does not indicate an effect of treatment, but rather a relationship between overall SGC survival and modulation depth irrespective of treatment. This strengthens the potential for using this specific relationship as an indicator of neural health in general.

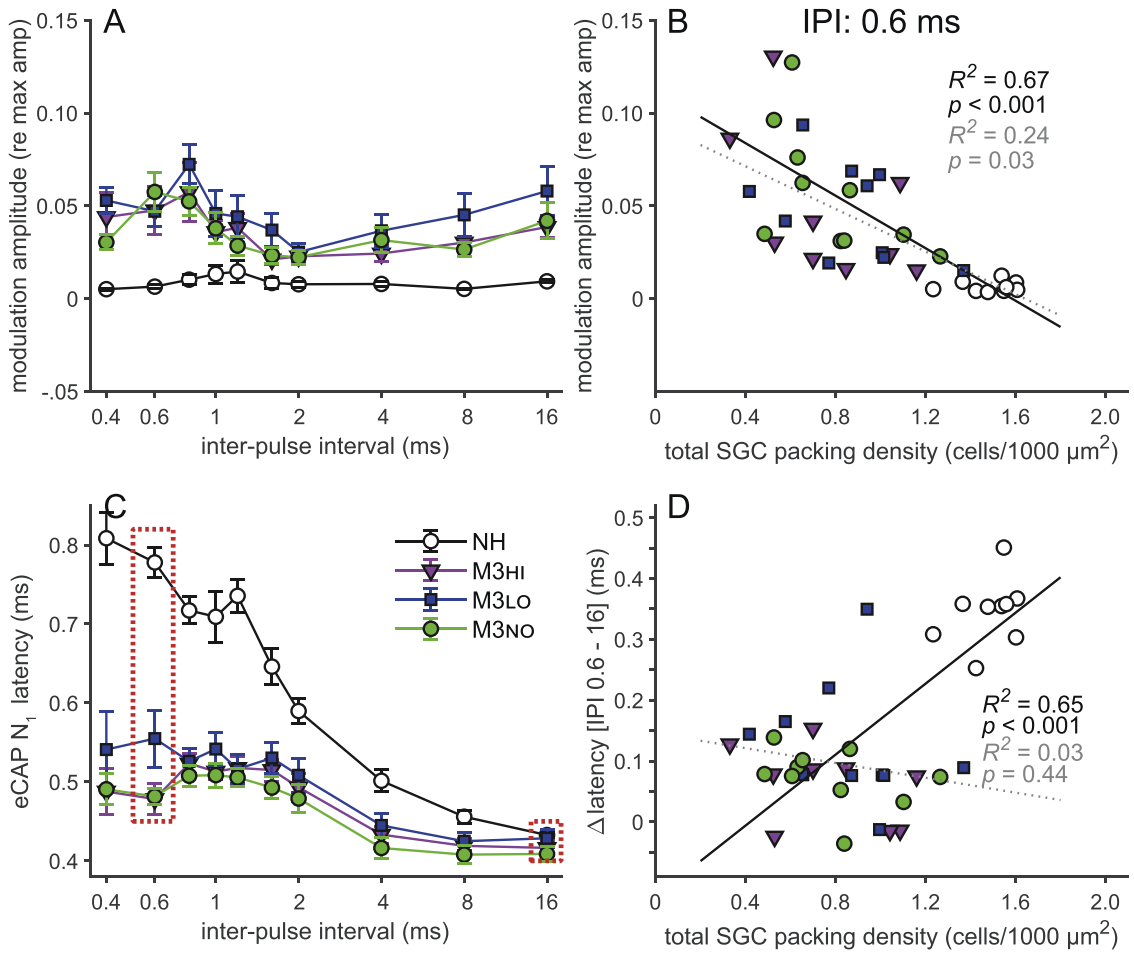

Fig. 13. Pulse-train response parameters. (A) Group means of normalized modulation depth determined for last 10 pulses of the 100 ms pulse train as a function of IPI. (B) Group means of eCAP N_1 latency averaged over the last 10 pulses of the 100 ms pulse train as a function of IPI. (C) Modulation depth for 0.6-ms IPI for individual animals as a function of basal SGC packing density. The black regression line and parameters are based on untreated (NH and M3NO) animals only, the dotted grey regression line and parameters are based on both treatment groups. (D) The difference in N_1 latency between 0.6-ms IPI and 16-ms IPI (dashed boxes in B) as function of basal spiral ganglion cell packing density. The black regression line and parameters are based on untreated (NH and M3NO) animals only, the dotted grey regression line and parameters are based on both treatment groups. NH, $n = 9$; M3HI, $n = 9$; M3LO, $n = 10$; M3NO, $n = 10$ animals. IPI, inter-pulse interval. Error bars represent SEM.

The outcomes from both recording paradigms would indicate that the treatment with M3 presented here is not able to mimic BDNF in terms of functional preservation. This lack of a functional effect could in part be due to the limited structural preservation observed following the M3 treatment, especially when compared to previously reported survival paired with an effect in the eCAP measures following treatment with BDNF. In addition, BDNF in the cochlea has a broader effect on the SGCs than merely preserving them. For instance, treatment with BDNF has been reported to increase SGC soma size (e.g. Ernfors et al., 1996; Shepherd et al., 2005; Glueckert et al., 2008; Agterberg et al., 2009; Leake et al., 2011; Ramekers et al., 2015a; Vink et al., 2021), potentially affecting functionality. An increase in soma size was not observed following M3-treatment (data not shown). In addition, BDNF is found to affect voltage-gated ion channel distribution on SGCs, increasing expression of ion channels related to rapid adaptation and brief response latencies (Adamson et al., 2002), which influences cellular activation. As such, the structural and functional preservation observed in previous studies with BDNF may have coincided as BDNF affects both aspects of cellular survival. The lack of significant effects on neural responsiveness may be explained by the several aspects in which M3 differs from BDNF such as binding to p75NTR and molecular weight. On the other hand, we cannot exclude the possibility that the various eCAP variables we applied using IPG variation and pulse train stimulation (Figs. 11–13) are not sensitive enough to measure small enhancements in neural survival as produced by M3 treatment. Nonetheless, M3 treatment clearly did not affect the neural excitation properties – irrespective of enhanced survival.

4.3. Therapeutic application

In vitro M3 was found to be a TrkB agonist, and as such was able to mimic the preservative effects of BDNF. In the present study, M3 treatment is found to result in less auditory nerve preservation in terms of cellular survival and functional preservation than that with BDNF treatment. Both of which are vital for CI usage, as a CI relies on an intact auditory nerve in order to properly function.

Besides cellular preservation, observed effects *in vitro* included the reparation of synapses in a synaptopathy model and neurite outgrowth (Szobota et al., 2019). Neither synapse repair nor PP outgrowth could be examined in the present study due study design limitations. However, in the present study we have observed limited *in vivo* preservation of SGCs and even less preservation of PPs, following treatment with M3. As reparation of synapses depends on the presence of PPs and these are not well preserved, it can thus be argued that synapse repair is unlikely to play a role of importance in clinical use. On the other hand, the model in the present study is one of induced deafness, based on damaging and

destroying cochlear hair cells. Therefore, any PP that would have the potential to have synapses repaired due to M3, would have limited to no inner hair cells to connect to. Promotion of outgrowth could also be functionally important for CI users, as regrown PPs – being the natural excitation points for the SGCs – can grow towards the CI and reduce the distance between the electrode and possibly the stimulation target which could reduce the CI stimulation current required and thereby increase frequency resolution. Recent studies have reported extensive outgrowth in response to BDNF in explant cultures (Szobota et al., 2019; Frick et al., 2020; Schmidbauer et al., 2023), with M3 being approximately 70% as effective as BDNF (Szobota et al., 2019). In the present study, treatment with M3 did not result in significantly higher PP/SGC ratio than the untreated control group, providing no evidence of potential outgrowth. Furthermore, M3 is approximately 35% as effective in SGC preservation as BDNF (given the BDNF AD/AS ratio of 2.12, or 112%, and the M3HI AD/AS ratio of 1.4, or 40% survival compared to the contralateral ear), which means that a potential positive effect by any outgrowth caused by M3 is unlikely to be relevant.

4.4. Blinding

In the present study, experimenters were blinded both during the experimental procedures as well as during the SGC and single-pulse eCAP analyses. While such a design is certainly not uncommon, it is rarely reported as such in the field of auditory animal research. This was also a novelty in our lab, as experimenters were usually only blinded during the data analysis. As far as we have been able to discover, in the past 40 years, not a single study exists in which experimenters are reportedly blind to both the intervention and the subsequent analyses. While such blinding is not always required, it will prevent possible intervention bias. Since the inception of the ARRIVE guidelines for improving the reporting of animal research (Kilkenny et al., 2010), its implementation has been limited (Bezdjian et al., 2018). With the guidelines recently updated (Percie du Sert et al., 2020) we feel that renewed attention to these are in place.

5. Conclusion

In this study we examined the preservative effects of the TrkB selective monoclonal antibody agonist M3 on the auditory nerve in the ototoxically deafened guinea pig. Treatment with M3 resulted in limited cellular survival, which was not accompanied by a treatment effect in the functional measurements. While the limited survival did include preservation in the middle and apical turns, which was not observed following treatment with BDNF or NT-3, the overall preservative effect of M3 is smaller than the outcomes following treatment with BDNF and NT-3. Under the present experimental conditions, the preservation of the auditory nerve produced by M3 was less robust than that of BDNF, particularly in terms of functional improvements. However, this picture could change with optimization of sustained cochlear delivery for M3 and other neurotrophin mimetics.

CRediT authorship contribution statement

Henk A. Vink: Investigation, Formal analysis, Software, Visualization, Writing – original draft, Writing – review & editing, Data curation. **Dyan Ramekers:** Conceptualization, Investigation, Software, Visualization, Writing – review & editing, Supervision. **Alan C. Foster:** Conceptualization, Resources, Methodology, Writing – review & editing. **Huib Versnel:** Conceptualization, Formal analysis, Writing – review & editing, Supervision, Project administration.

Data availability

Data will be made available on request.

Acknowledgments

We would like to thank Ferry Hendriksen for histological processing and analysis, Anouk van den Brink, Raishna Biharie, Thomas Ootjers, and Yexin Ye for assisting in SGC quantification, and Glauco Cristofaro and Anat Bouwmeester for surgical assistance. Additionally, we thank MED-EL GmbH, Innsbruck, Austria, for eCAP recording equipment and technical support.

References

Adamson, C.L., Reid, M.A., Davis, R.L., 2002. Opposite actions of brain-derived neurotrophic factor and neurotrophin-3 on firing features and ion channel composition of murine spiral ganglion neurons. J. Neurosci. 22, 1385–1396. https://doi.org/10.1523/JNEUROSCI.22-04-01385.2002.

Agterberg, M.J.H., Versnel, H., van Dijk, L.M., de Groot, J.C.M.J., Klis, S.F.L., 2009. Enhanced survival of spiral ganglion cells after cessation of treatment with brain-derived neurotrophic factor in deafened guinea pigs. J. Assoc. Res. Otolaryngol. 10, 355–367. https://doi.org/10.1007/s10162-009-0170-2.

Bezdjian, A., Klis, S.F.L., Peters, J.P.M., Grolman, W., Stegeman, I., 2018. Quality of reporting of otorhinolaryngology articles using animal models with the ARRIVE statement. Lab. Anim. 52, 79–87. https://doi.org/10.1177/0023677217718862.

Brahimi, F., Galan, A., Siegel, S., Szobota, S., Sarunic, M.V., Foster, A.C., Saragovi, H.U., 2021. Therapeutic neuroprotection by an engineered neurotrophin that selectively activates tropomyosin receptor kinase (Trk) family neurotrophin receptors but not the p75 neurotrophin receptor. Mol. Pharmacol. 100, 491–501. https://doi.org/10.1124/molpharm.121.000301.

Bronfman, F.C., Escudero, C.A., Weis, J., Kruttgen, A., 2007. Endosomal transport of neurotrophins: roles in signaling and neurodegenerative diseases. Dev. Neurobiol. 67, 1183–1203. https://doi.org/10.1002/dneu.20513.

Budenz, C.L., Wong, H.T., Swiderski, D.L., Shibata, S.B., Pfingst, B.E., Raphael, Y., 2015. Differential effects of AAV.BDNF and AAV.Ntf3 in the deafened adult guinea pig ear. Sci. Rep. 5, 8619. https://doi.org/10.1038/srep08619.

Canossa, M., Griesbeck, O., Berninger, B., Campana, G., Kolbeck, R., Thoenen, H., 1997. Neurotrophin release by neurotrophins: implications for activity-dependent neuronal plasticity. Proc. Natl. Acad. Sci. U. S. A. 94, 13279–13286. https://doi.org/10.1073/pnas.94.24.13279.

Chao, M.V., 2003. Neurotrophins and their receptors: a convergence point for many signalling pathways. Nat. Rev. Neurosci. 4, 299–309. https://doi.org/10.1038/nrn1078.

Ernfors, P., Li Duan, M., Elshamy, W.M., Canlon, B., 1996. Protection of auditory neurons from aminoglycoside toxicity by neurotrophin-3. Nat. Med. 2, 463–467. https://doi.org/10.1038/nm0496-463.

Foster, A.C., Szobota, S., Piu, F., Jacques, B.E., Moore, D.R., Sanchez, V.A., Anderson, J. J., 2022. A neurotrophic approach to treating hearing loss: Translation from animal models to clinical proof-of-concept. J. Acoust. Soc. Am. 151, 3937–3946. https://doi.org/10.1121/10.0011510.

Frick, C., Fink, S., Schmidbauer, D., Rousset, F., Eickhoff, H., Tropitzsch, A., Kramer, B., Senn, P., Glueckert, R., Rask-Andersen, H., Wiesmüller, K.H., Löwenheim, H., Müller, M., 2020. Age-dependency of neurite outgrowth in postnatal mouse cochlear spiral ganglion explants. Brain Sci. 10, 580. https://doi.org/10.3390/brainsci10090580.

Fritzsch, B., Tessarollo, L., Coppola, E, Reichardt, L.F., 2004. Neurotrophins in the ear: their roles in sensory neuron survival and fiber guidance. Prog. Brain Res. 146, 265–278. https://doi.org/10.1016/S0079-6123(03)46017-2.

Gillespie, L.N., Clark, G.M., Marzella, P.L., 2004. Delayed neurotrophin treatment supports auditory neuron survival in deaf guinea pigs. Neuroreport 15, 1121–1125. https://doi.org/10.1097/00001756-200405190-00008.

Glueckert, R., Bitsche, M., Miller, J.M., Zhu, Y., Prieskorn, D.M., Altschuler, R.A., Schrott-Fischer, A., 2008. Deafferentiation-associated changes in afferent and efferent processes in the guinea pig cochlea and afferent regeneration with chronic intrascalar brain-derived neurotrophic factor and acidic fibroblast growth factor. J. Comp. Neurol. 507, 1602–1621. https://doi.org/10.1002/cne.21619.

Green, S.H., Bailey, E., Wang, Q., Davis, R.L., 2012. The Trk A, B, C's of neurotrophins in the cochlea. Anat. Rec. 295, 1877–1895. https://doi.org/10.1002/ar.22587. Hoboken.

Havenith, S., Versnel, H., Klis, S.F.L., Grolman, W., 2015. Local delivery of brain-derived neurotrophic factor on the perforated round window membrane in guinea pigs: a possible clinical application. Otol. Neurotol. 36, 705–713. https://doi.org/10.1097/MAO.0000000000000634.

Howe, C.L., Mobley, W.C., 2004. Signaling endosome hypothesis: a cellular mechanism for long distance communication. J. Neurobiol. 58, 207–216. https://doi.org/10.1002/neu.10323.

Huang, E.J., Reichardt, L.F., 2001. Neurotrophins: roles in neuronal development and function. Annu. Rev. Neurosci. 24, 677–736. https://doi.org/10.1146/annurev.neuro.24.1.677.

Huang, EJ, Reichardt, LF, 2003. Trk receptors: roles in neuronal signal transduction. Annu. Rev. Biochem. 72, 609–642. https://doi.org/10.1146/annurev.biochem.72.121801.161629.

Jang, S.W., Liu, X., Yepes, M., Shepherd, K.R., Miller, G.W., Liu, Y., Wilson, W.D., Xiao, G., Blanchi, B., Sun, Y.E., Ye, K., 2010a. A selective TrkB agonist with potent neurotrophic activities by 7,8-dihydroxyflavone. Proc. Natl. Acad. Sci. 107, 2687–2692. https://doi.org/10.1073/pnas.0913572107.

Jang, S.W., Liu, X., Pradoldej, S., Tosini, G., Chang, Q., Iuvone, P.M., Ye, K., 2010b. N-acetylserotonin activates TrkB receptor in a circadian rhythm. Proc. Natl. Acad. Sci. 107, 3876–3881. https://doi.org/10.1073/pnas.0912531107.

Jang, S.W., Liu, X., Chan, C.B., France, S.A., Sayeed, I., Tang, W., Lin, X., Xiao, G., Andero, R., Chang, Q., Ressler, K.J., Ye, K., 2010c. Deoxygedunin, a natural product with potent neurotrophic activity in mice. PLOS One 5, e11528. https://doi.org/10.1371/journal.pone.0011528.

Ji, Y., Lu, Y., Yang, F., Shen, W., Tang, T.T., Feng, L., Duan, S., Lu, B., 2010. Acute and gradual increases in BDNF concentration elicit distinct signaling and functions in neurons. Nat. Neurosci. 13, 302–309. https://doi.org/10.1038/nn.2505.

Kamakura, T., Nadol, J.B., 2016. Correlation between word recognition score and intracochlear new bone and fibrous tissue after cochlear implantation in the human. Hear. Res. 339, 132–141. https://doi.org/10.1016/j.heares.2016.06.015.

Kersigo, J., Pan, N., Lederman, J.D., Chatterjee, S., Abel, T., Pavlinkova, G., Silos-Santiago, I., Fritzsch, B., 2018. A RNAscope whole mount approach that can be combined with immunofluorescence to quantify differential distribution of mRNA. Cell Tissue Res. 374, 251–262. https://doi.org/10.1007/s00441-018-2864-4.

Kilkenny, C., Browne, W.J., Cuthill, I.C., Emerson, M., Altman, D.G., 2010. Improving bioscience research reporting: the ARRIVE guidelines for reporting animal research. PLOS Biol. 8, e1000412 https://doi.org/10.1371/journal.pbio.1000412.

Kujawa, S.G., Liberman, M.C., 2015. Synaptopathy in the noise-exposed and aging cochlea: Primary neural degeneration in acquired sensorineural hearing loss. Hear. Res. 330, 191–199. https://doi.org/10.1016/j.heares.2015.02.009.

Landry, T.G., Wise, A.K., Fallon, J.B., Shepherd, R.K., 2011. Spiral ganglion neuron survival and function in the deafened cochlea following chronic neurotrophic treatment. Hear. Res. 282, 303–313. https://doi.org/10.1016/j.heares.2011.06.007.

Leake, P.A., Hradek, G.T., 1988. Cochlear pathology of long term neomycin induced deafness in cats. Hear. Res. 33, 11–33. https://doi.org/10.1016/0378-5955(88)90018-4.

Leake, P.A., Hradek, G.T., Hetherington, A.M., Stakhovskaya, O., 2011. Brain-derived neurotrophic factor promotes cochlear spiral ganglion cell survival and function in deafened, developing cats. J. Comp. Neurol. 519, 1526–1545. https://doi.org/10.1002/cne.22582.

Liu, X., Chan, C., Jang, S., Pradoldej, S., Huang, J, He, K., Phun, L.H., France, S., Xiao, G., Jia, Y., Luo, H.R., Ye, K., 2010. A Synthetic 7,8-Dihydroxyflavone Derivative Promotes Neurogenesis and Exhibits Potent Antidepressant Effect. J. Med. Chem. 53, 8274–8286. https://doi.org/10.1021/jm101206p.

Longo, F.M., Massa, S.M., 2013. Small-molecule modulation of neurotrophin receptors: a strategy for the treatment of neurological disease. Nat. Rev. Drug Discov. 12, 507–525. https://doi.org/10.1038/nrd4024.

Massa, S.M., Yang, T., Xie, Y., Shi, J., Bilgen, M., Joyce, J.N., Nehama, D., Rajadas, J., Longo, F.M., 2010. Small molecule BDNF mimetics activate TrkB signaling and prevent neuronal degeneration in rodents. J. Clin. Invest. 120, 1774–1785. https://doi.org/10.1172/JCI41356.

Miller, J.M., Chi, D.H., O'Keeffe, L.J., Kruszka, P., Raphael, Y., Altschuler, R.A., 1997. Neurotrophins can enhance spiral ganglion cell survival after inner hair cell loss. Int. J. Dev. Neurosci. 15, 631–643. https://doi.org/10.1016/S0736-5748(96)00117-7.

Miller, J.M., Le Prell, C.G., Prieskorn, D.M., Wys, N.L., Altschuler, R.A., 2007. Delayed neurotrophin treatment following deafness rescues spiral ganglion cells from death and promotes regrowth of auditory nerve peripheral processes: Effects of brain-derived neurotrophic factor and fibroblast growth factor. J. Neurosci. Res. 85, 1959–1969. https://doi.org/10.1002/jnr.21320.

Percie du Sert, N., Ahluwalia, A., Alam, S., Avey, M.T., Baker, M., Browne, W.J., Clark, A., Cuthill, I.C., Dirnagl, U., Emerson, M., Garner, P., Holgate, S.T., Howells, D.W., Hurst, V., Karp, N.A., Lazic, S.E., Lidster, K., MacCallum, C.J., Macleod, M., Pearl, E.J., Petersen, O.H., Rawle, F., Reynolds, P., Rooney, K., Sena, E. S., Silberberg, S.D., Steckler, T., Würbel, H., 2020. Reporting animal research: Explanation and elaboration for the ARRIVE guidelines 2.0. PLoS Biol. 18, e3000411 https://doi.org/10.1371/journal.pbio.3000411.

Prado-Guitierrez, P., Fewster, L.M., Heasman, J.M., McKay, C.M., Shepherd, R.K., 2006. Effect of interphase gap and pulse duration on electrically evoked potentials is correlated with auditory nerve survival. Hear. Res. 215, 47–55. https://doi.org/10.1016/j.heares.2006.03.006.

Ramekers, D., Versnel, H., Grolman, W., Klis, S.F.L., 2012. Neurotrophins and their role in the cochlea. Hear. Res. 288, 19–33. https://doi.org/10.1016/j.heares.2012.03.002.

Ramekers, D., Versnel, H., Strahl, S.B., Smeets, E.M., Klis, S.F.L., Grolman, W., 2014. Auditory-nerve responses to varied inter-phase gap and phase duration of the electric pulse stimulus as predictors for neuronal degeneration. J. Assoc. Res. Otolaryngol. 15, 187–202. https://doi.org/10.1007/s10162-013-0440-x.

Ramekers, D., Versnel, H., Strahl, S.B., Klis, S.F.L., Grolman, W., 2015a. Temporary neurotrophin treatment prevents deafness-induced auditory nerve degeneration and preserves function. J. Neurosci. 35, 12331–12345. https://doi.org/10.1523/JNEUROSCI.0096-15.2015.

Ramekers, D., Versnel, H., Strahl, S.B., Klis, S.F.L., Grolman, W., 2015b. Recovery characteristics of the electrically stimulated auditory nerve in deafened guinea pigs: relation to neuronal status. Hear. Res. 321, 12–24. https://doi.org/10.1016/j.heares.2015.01.001.

Ramekers, D., Klis, S.F.L., Versnel, H., 2020. Simultaneous rather than retrograde spiral ganglion cell degeneration following ototoxically induced hair cell loss in the guinea pig cochlea. Hear. Res. 390, 107928 https://doi.org/10.1016/j.heares.2020.107928.

Ramekers, D., Benav, H., Klis, S.F.L., Versnel, H., 2022. Changes in the electrically evoked compound action potential over time after implantation and subsequent deafening in guinea pigs. J. Assoc. Res. Otolaryngol. https://doi.org/10.1007/s10162-022-00864-0.

Richardson, R.T., Hu, Q.Y., Shi, F., Nguyen, T., Fallon, J.B., Flynn, B.O., Wise, A.K., 2019. Pharmacokinetics and tissue distribution of neurotrophin 3 after intracochlear delivery. J. Control. Release 299, 53–63. https://doi.org/10.1016/j.jconrel.2019.02.018.

Saragovi, H.U., Galan, A., Levin, L.A., 2019. Neuroprotection: Pro-survival and anti-neurotoxic mechanisms as therapeutic strategies in neurodegeneration. Front. Cell. Neurosci. 13, 231. https://doi.org/10.3389/fncel.2019.00231.

Scheper, V., Seidel-Effenberg, I., Lenarz, T., Stöver, T., Paasche, G., 2020. Consecutive treatment with brain-derived neurotrophic factor and electrical stimulation has a protective effect on primary auditory neurons. Brain Sci. 10, 559. https://doi.org/10.3390/brainsci10080559.

Schimmang, T., Tan, J., Müller, M., Zimmermann, U., Rohbock, K., Köpschall, I., Limberger, A., Minichiello, L., Knipper, M., 2003. Lack of Bdnf and TrkB signalling in the postnatal cochlea leads to a spatial reshaping of innervation along the tonotopic axis and hearing loss. Development 130, 4741–4750. https://doi.org/10.1242/dev.00676.

Schmidbauer, D., Fink, S., Rousset, F., Löwenheim, H., Senn, P., Glueckert, R., 2023. Closing the gap between the auditory nerve and cochlear implant electrodes: which neurotrophin cocktail performs best for axonal outgrowth and is electrical stimulation beneficial? Int. J. Mol. Sci. 24, 2013. https://doi.org/10.3390/ijms24032013.

Seyyedi, M, Viana, LM, Nadol, JB, 2014. Within-subject comparison of word recognition and spiral ganglion cell count in bilateral cochlear implant recipients. Otol. Neurotol. 35, 1446–1450. https://doi.org/10.1097/MAO.0000000000000443.

Shepherd, R.K., Hardie, N.A., 2001. Deafness-induced changes in the auditory pathway: implications for cochlear implants. Audiol. Neuro Otol. 6, 305–318. https://doi.org/10.1159/000046843.

Shepherd, R.K., Javel, E., 1997. Electrical stimulation of the auditory nerve. I. Correlation of physiological responses with cochlear status. Hear. Res. 108, 112–144. https://doi.org/10.1016/S0378-5955(97)00046-4.

Shepherd, R.K., Coco, A., Epp, S.B., Crook, J.M., 2005. Chronic depolarization enhances the trophic effects of brain-derived neurotrophic factor in rescuing auditory neurons following a sensorineural hearing loss. J. Comp. Neurol. 486, 145–158. https://doi.org/10.1002/cne.20564.

Sly, D.J., Campbell, L., Uschakov, A., Saief, S.T., Lam, M., O'Leary, S.J., 2016. Applying neurotrophins to the round window rescues auditory function and reduces inner hair cell synaptopathy after noise-induced hearing loss. Otol. Neurotol. 37, 1223–1230. https://doi.org/10.1097/MAO.0000000000001191.

Spoendlin, H., 1975. Retrograde degeneration of the cochlear nerve. Acta Otolaryngol. 79, 266–275. https://doi.org/10.3109/00016487509124683.

Spoendlin, H., 1985. Anatomy of Cochlear Innervation. Am. J. Otolaryngol. Neck Med. Surg. 6, 453–467. https://doi.org/10.1016/S0196-0709(85)80026-0.

Staecker, H., Kopke, R., Malgrange, B., Lefebvre, P., Van De Water, T.R., 1996. NT-3 and/or BDNF therapy prevents loss of auditory neurons following loss of hair cells. Neuroreport 7, 889–894. https://doi.org/10.1097/00001756-199603220-00011.

Sugawara, M., Murtie, J.C., Stankovic, K.M., Liberman, M.C., Corfas, G., 2007. Dynamic patterns of neurotrophin 3 expression in the postnatal mouse inner ear. J. Comp. Neurol. 501, 30–37. https://doi.org/10.1002/cne.21227.

Szobota, S., Mathur, P.D., Siegel, S., Black, K., Saragovi, H.U., Foster, A.C., 2019. BDNF, NT-3 and Trk receptor agonist monoclonal antibodies promote neuron survival, neurite extension, and synapse restoration in rat cochlea ex vivo models relevant for hidden hearing loss. PLOS One 14, e0224022. https://doi.org/10.1371/journal.pone.0224022.

Tisi, A., Rovers, J., Vink, H.A., Ramekers, D., Maccarone, R., Versnel, H., 2022. No protective effects of hair cells or supporting cells in ototoxically deafened guinea pigs upon administration of BDNF. Brain Sci 12, 2. https://doi.org/10.3390/brainsci12010002.

Tsivkovskaia, N, Fernandez, C, Altmann, T, Fernandez, R, Wang, X, Mathur, P, Siegel, S, Szobota, S, Uribe, P, Stepanenko, A, Jacques, B, Foster, A, Piu, F, 2021. Characterization of aTrkB mAb agonist for the treatment of hearing loss due to cochlear synaptopathy. In: Proceedings of the Presented at: Association for Research in Otolaryngology Mid-winter Meeting.

Van Loon, M.C., Ramekers, D., Agterberg, M.J.H., de Groot, J.C.M.J., Grolman, W., Klis, S.F.L., Versnel, H., 2013. Spiral ganglion cell morphology in guinea pigs after deafening and neurotrophic treatment. Hear. Res. 298, 17–26. https://doi.org/10.1016/j.heares.2013.01.013.

Versnel, H, Agterberg, MJH, de Groot, JCMJ, Smoorenburg, GF, Klis, SFL, 2007. Time course of cochlear electrophysiology and morphology after combined administration of kanamycin and furosemide. Hear. Res. 231, 1–12. https://doi.org/10.1016/j.heares.2007.03.003.

Vink, H.A., van Dorp, W.C., Thomeer, H.G.X.M., Versnel, H., Ramekers, D., 2020. BDNF outperforms TrkB agonist 7,8,3′-THF in preserving the auditory nerve in deafened Guinea pigs. Brain Sci 10, 787. https://doi.org/10.3390/brainsci10110787.

Vink, H.A., Versnel, H., Kroon, S., Klis, S.F.L., Ramekers, D., 2021. BDNF-mediated preservation of spiral ganglion cell peripheral processes and axons in comparison to that of their cell bodies. Hear. Res. 400, 108114 https://doi.org/10.1016/j.heares.2020.108114.

Vink, H.A., Ramekers, D., Thomeer, H.G.X.M., Versnel, H., 2022. Combined brain-derived neurotrophic factor and neurotrophin-3 treatment is preferred over either one separately in the preservation of the auditory nerve in deafened guinea pigs. Front. Mol. Neurosci. 15, 935111 https://doi.org/10.3389/fnmol.2022.935111.

Waaijer, L., Klis, S.F.L., Ramekers, D., Van Deurzen, M.H.W., Hendriksen, F.G.J., Grolman, W., 2013. The peripheral processes of spiral ganglion cells after intracochlear application of brain-derived neurotrophic factor in deafened guinea pigs. Otol. Neurotol. 34, 570–578. https://doi.org/10.1097/MAO.0b013e31828687b1.

Webster, M., Webster, D.B., 1981. Spiral ganglion neuron loss following organ of Corti loss: A quantitative study. Brain Res. 212, 17–30. https://doi.org/10.1016/0006-8993(81)90028-7.

Wise, AK, Richardson, R, Hardman, J, Clark, G, O'Leary, S, 2005. Resprouting and survival of Guinea pig cochlear neurons in response to the administration of the neurotrophins brain-derived neurotrophic factor and neurotrophin-3. J. Comp. Neurol. 487, 147e165. https://doi.org/10.1002/cne.20563.

Wise, A.K., Tan, J., Wang, Y., Caruso, F., Shepherd, R.K., 2016. Improved auditory nerve survival with nanoengineered supraparticles for neurotrophin delivery into the deafened cochlea. PLOS One 11, e0164867. https://doi.org/10.1371/journal.pone.0164867.

Wu, PZ, O'Malley, JT, de Gruttola, V, Liberman, MC, 2021. Primary neural degeneration in noise-exposed human cochleas: Correlations with outer hair cell loss and word-discrimination scores. J. Neurosci. 41, 4439–4447. https://doi.org/10.1523/JNEUROSCI.3238-20.2021.

Yang, T., Massa, S.M., Tran, K.C., Simmons, D.A., Rajadas, J., Zeng, A.Y., Jang, T., Carsanaro, S., Longo, F.M., 2016. A small molecule TrkB/TrkC neurotrophin receptor co-activator with distinctive effects on neuronal survival and process outgrowth. Neuropharmacology 110. https://doi.org/10.1016/j.neuropharm.2016.06.015.

Ylikoski, J, Wersäll, J, Björkroth, B, 1974. Degeneration of neural elements in the cochlea of the guinea-pig after damage to the organ of Corti by ototoxic antibiotics. Acta Otolaryngol. 78, 23–41. https://doi.org/10.3109/00016487409129730.

Yu, Q., Chang, Q., Liu, X., Gong, S., Ye, K., Lin, X., 2012. 7,8,3′-Trihydroxyflavone, a potent small molecule TrkB receptor agonist, protects spiral ganglion neurons from degeneration both *in vitro* and *in vivo*. Biochem. Biophys. Res. Commun. 422, 387–392. https://doi.org/10.1016/j.bbrc.2012.04.154.

Yu, Q., Chang, Q., Liu, X., Wang, Y., Li, H., Gong, S., Ye, K., Lin, X., 2013. Protection of spiral ganglion neurons from degeneration using small-molecule TrkB receptor agonists. J. Neurosci. 33, 13042–13052. https://doi.org/10.1523/JNEUROSCI.0854-13.2013.

Zilberstein, Y., Liberman, M.C., Corfas, G., 2012. Inner hair cells are not required for survival of spiral ganglion neurons in the adult cochlea. J. Neurosci. 32, 405–410. https://doi.org/10.1523/JNEUROSCI.4678-11.2012.